# IMPLICATIONS OF NON-MAXWELLIAN DISTRIBUTIONS ON BIG BANG NUCLEOSYNTHESIS

A Thesis

by

JOHN FUQUA

Submitted to the Office of Graduate Studies
Texas A&M University-Commerce
In partial fulfillment of the requirements
for the degree of
MASTER OF SCIENCE
May 2013

# IMPLICATIONS OF NON-MAXWELLIAN DISTRIBUTIONS ON BIG BANG NUCLEOSYNTHESIS

A Thesis

by

JOHN FUQUA

Approved by:

| | |
|---|---|
| Advisor: | Carlos Bertulani |
| Committee: | Kurtis Williams<br>Bao-An Li<br>Carlos Bertulani |
| Head of Department: | Matt Wood |
| Dean of the College: | Grady Blount |
| Dean of Graduate Studies: | Arlene Horne |

# ABSTRACT

## IMPLICATIONS OF NON-MAXWELLIAN DISTRIBUTIONS ON BIG BANG NUCLEOSYNTHESIS

John Fuqua, MS
Texas A&M University-Commerce, 2013

Advisor: Carlos Bertulani, PhD A model was constructed by physicists to predict the abundance of the light elements produced during a period of time known as big bang nucleosynthesis epoch. Today we can observe these values and compare them to the predictions. The model has been very accurate for many of the abundances, but there are still some discrepancies. While there are many possible solutions, we consider a different statistical approach to solving the rates at which the elements are produced and destroyed.

In this work the abundances of light elements based on the big bang nucleosynthesis model are calculated using the Tsallis non-extensive statistics. The impact of the variation of the non-extensive parameter $q$ from the unity value is compared to observations and to the abundance yields from the standard big bang model. We find large differences between the reaction rates and the abundances of light elements calculated with the extensive and the non-extensive statistics. But a large deviation of the non-extensive parameter from $q = 1$ (corresponding to Boltzmann statistics) does not seem to be compatible with observations (C. A. Bertulani, Fuqua, & Hussein, 2013).

# ACKNOWLEDGEMENTS

The challenges set forth by Dr. Carlos Bertulani have stimulated my interest in and outside of the classroom. His patience, honesty and friendship are highly valued and have contributed to my understanding not just in physics but in other areas as well. I am very fortunate my experiences have been complimented by his mentorship. Without his assistance my graduate project would not be possible and I sincerely appreciate everything he has done for me.

Furthermore, I would like to thank Mahir Hussein for his contributions to the development and progression of the project.

I would also like to thank Dr. Bao-An Li for the enthusiasm he brought into the classroom and for finding scholarships that ensured my financial stability.

Additionally, I am thankful to my friends who have enriched my learning experiences and have offered their support. In particular I would like to thank Joshua Hooker for the many thought provoking and fun discussions.

My parents have played key roles in my life and have always been there to encourage, support and at times discipline me. I am very thankful for their influence which has taught me so much and has led me to where I am today.

Lastly, I am grateful to the Department of Physics and Astronomy for offering me the role of teaching assistant which has broadened my views. I also appreciate the National Science Foundation for their STEM program and Texas A&M University-Commerce Graduate School for their financial support.

TABLE OF CONTENTS

# LIST OF TABLES

# LIST OF FIGURES

# CHAPTER 1
# INTRODUCTION

The cosmological big bang model is in agreement with many observations relevant for our understanding of the universe. However, comparison of calculations based on the model with observations is not straightforward because the data are subject to poorly known evolutionary effects and systematic errors. Nonetheless, the model is believed to be the only probe of physics in the early universe during the interval from $3 - 20$ min, after which the temperature and density of the universe fell below that which is required for nuclear fusion and prevented elements heavier than beryllium from forming. The model is inline with the cosmic microwave background (CMB) radiation temperature of 2.275 K (P. Noterdaeme, 2011), and provides guidance to other areas of science, such as nuclear and particle physics. Big bang model calculations are also consistent with the number of light neutrino families $N_\nu = 3$. According to the numerous literature on the subject, the big bang model can accommodate values between $N_\nu = 1.8 - 3.9$ [see, e.g., Olive (2002)]. From the measurement of the $Z_0$ width by LEP experiments at CERN one knows that $N_\nu = 2.9840 \pm 0.0082$ (Collaboration, 2006).

In the big bang model nearly all neutrons end up in $^4$He, so that the relative abundance of $^4$He depends on the number of neutrino families and also on the neutron lifetime $\tau_n$. The sensitivity to the neutron lifetime affects Big Bang Nucleosynthesis (BBN) in two ways. The neutron lifetime $\tau_n$ influences the weak reaction rates because of the relation between $\tau_n$ and the weak coupling constant. A shorter (longer) $\tau_n$ means that the reaction rates remain greater (smaller) than the Hubble expansion rate until a lower (larger) freeze-out temperature, having a strong impact on the equilibrium neutron-to-proton ratio at freeze-out. This $n/p$-ratio is approximately given in thermal equilibrium by $n/p = \exp[-\Delta m/k_B T] \sim 1/6$, where $k_B$ is the Boltzmann constant, $T$ the temperature at weak freeze-out, and $\Delta m$ is the neutron-proton mass difference. The other influence of $\tau_n$ is due to their decay in the interval between weak freeze-out ($t \sim 1$ s) and when nucleosynthesis starts ($t \sim 200$ s), reducing the $n/p$ ratio to $n/p \sim 1/7$. A shorter $\tau_n$ implies lower the predicted BBN helium

abundance. In this work we will use the value of $\tau_n = 878.5 \pm 0.7 \pm 0.3$ s, according to the most recent experiments by A. Serebrov (2005) [a recent review on the neutron lifetime is found in Wietfeldt and Greene (2011)]. Recently, the implications of a change in the neutron lifetime on BBN predictions have been assessed by Mathews, Kajino, and Shima (2005).

The baryonic density of the universe deduced from the observations of the anisotropies of the CMB radiation, constrains the value of the number of baryons per photon, $\eta$, which remains constant during the expansion of the universe. Big bang model calculations are compatible with the experimentally deduced value of from WMAP observations, $\eta = 6.16 \pm 0.15 \times 10^{-10}$ (Komatsu, 2011).

Of our interest in this work is the abundance of light elements in big bang nucleosynthesis. At the very early stages (first 20 min) of the universe evolution, when it was dense and hot enough for nuclear reactions to take place, the temperature of the primordial plasma decreased from a few MeV down to about 10 keV, light nuclides as $^2$H, $^3$He, $^4$He and, to a smaller extent, $^7$Li were produced via a network of nuclear processes, resulting into abundances for these species which can be determined with several observational techniques and in different astrophysical environments. Apparent discrepancies for the Li abundances in metal poor stars, as measured observationally and as inferred by WMAP, have promoted a wealth of new inquiries on BBN and on stellar mixing processes destroying Li, whose results are not yet final. Further studies of light-element abundances in low metallicity stars and extragalactic H II regions, as well as better estimates from BBN models are required to tackle this issue, integrating high resolution spectroscopic studies of stellar and interstellar matter with nucleosynthesis models and nuclear physics experiments and theories (Fields, 2011).

The Maxwell-Boltzmann distribution of the kinetic energy of the ions in a plasma is one of the basic inputs for the calculation of nuclear reaction rates during the BBN. The distribution is based on several assumptions inherent to the Boltzmann-Gibbs statistics: (a) the collision time is much smaller than the mean time between collisions, (b) the interaction is local, (c) the velocities of two particles at the same point are not correlated, and (d) that energy is locally conserved when using only the degrees of freedom of the colliding particles

(no significant amount of energy is transferred to and from collective variables and fields). If (a) and (b) are not valid the resulting effective two-body interaction is non-local and depends on the momentum and energy of the particles. Even when the one-particle energy distribution is Maxwellian, additional assumptions about correlations between particles are necessary to deduce that the relative-velocity distribution is also Maxwellian. Although the Boltzmann-Gibbs (BG) description of statistical mechanics is well established in a seemingly infinite number of situations, in recent years an increasing theoretical effort has concentrated on the development of alternative approaches to statistical mechanics which includes the BG statistics as a special limit of a more general theory (Tsallis, 1988) [see also, Rényi (1960)]. Such theories aim to describe systems with long range interactions and with memory effects (or non-ergodic systems). A very popular alternative to the BG statistics was proposed by C. Tsallis (Gell-Mann & Tsallis, 2004; Tsallis, 1988), herewith denoted as *non-extensive statistics* [for more details on this subject, see the extensive reviews C. Tsallis and Sato (2005); Gell-Mann and Tsallis (2004); Tsallis (2009)]. Statistical mechanics assumes that energy is an "extensive" variable, meaning that the total energy of the system is proportional to the system size; similarly the entropy is also supposed to be extensive. This might be justified due to the short-range nature of the interactions which hold matter together. But if one deals with long-range interactions, most prominently gravity; one can then find that entropy is not extensive (Chavanis & Sire, 2005; Fa & Lenzi, 2001; Lima, Silva, & Santos, 2002; Sakagami & Taruya, 2004; Taruya & Sakagami, 2003).

In classical statistics, to calculate the average values of some quantities, such as the energy of the system, the number of molecules, the volume it occupies, etc, one searches for the probability distribution which maximizes the entropy, subject to the constraint that it gives the right average values of those quantities. As mentioned above, Tsallis proposed to replace the usual (BG) entropy with a new, non-extensive quantity, now commonly called the *Tsallis entropy*, and maximize that, subject to the same usual constraints. There is actually a whole infinite family of Tsallis entropies, indexed by a real-valued parameter $q$, which quantifies the degree of departure from extensivity (one gets the usual entropy back again when $q = 1$). It was shown in many circumstances that the classical results of statistical

mechanics can be translated into the new theory (Tsallis, 2009). The importance of these families of entropies is that, when applied to ordinary statistical mechanics, they give rise to probabilities that follow power laws instead of the exponential laws of the standard case [for details on this see Tsallis (2009)]. In most cases that Tsallis formalism is adopted, e.g. Pessah, Torres, and Vucetich (2001), the non-extensive parameter $q$ is taken to be constant and close to the value for which ordinary statistical mechanics is obtained ($q = 1$). Some works have also probed sizable deviations of the non-extensive parameter $q$ from the unity to explain a variety of phenomena in several areas of science (Gell-Mann & Tsallis, 2004).

In the next sections, we shown that the Maxwell-Boltzmann distribution, a cornerstone of the big bang and stellar evolution nucleosynthesis, is strongly modified by the non-extensive statistics if $q$ strongly deviates from the unity. As a consequence, it also affects strongly the predictions of the BBN. There is no "a priori" justification for a large deviation of $q$ from the unity value during the BBN epoch. In particular, as radiation is assumed to be in equilibrium with matter during the BBN, a modification of the Maxwell distribution of velocities would also impact the Planck distribution of photons. Recent studies on the temperature fluctuations of the cosmic microwave background (CMB) radiation have shown that a modified Planck distribution based on Tsallis statistics adequately describes the CMB temperature fluctuations measured by WMAP with $q = 1.045 \pm 0.005$, which is close to unity but not quite (Bernui, Tsallis, & Villela, 2007). Perhaps more importantly, Gaussian temperature distributions based on the BG statistics, corresponding to the $q \to 1$ limit, do not properly represent the CMB temperature fluctuations (Bernui et al., 2007). Such fluctuations, allowing for even larger variations of $q$ might occur during the BBN epoch, also leading to a change of the exponentially decaying tail of the Maxwell velocity distribution.

Based on the successes of the big bang model, it is fair to assume that it can set strong constraints on the limits of the parameter $q$ used in a non-extensive statistics description of the Maxwell-Boltzmann velocity distribution. In the literature, attempts to solve the lithium problem has assumed all sorts of "new physics" (Fields, 2011). The present work adds to the list of new attempts, although our results imply a much wider impact on BBN as expected for the solution of the lithium problem. If the Tsallis statistics appropriately describes the

deviations of tails of statistical distributions, then the BNN would effectively probe such tails. The Gamow window (see Figure 3.1) contains a small fraction of the total area under the velocity distribution. Thus, only a few particles in the tail of the distributions contribute to the fusion rates. In fact, the possibility of a deviation of the Maxwellian distribution and implications of the modification of the Maxwellian distribution tail for nuclear burning in stars have already been explored in the past (Coraddu, 1999; Degl'Innocenti, Fiorentini, Lissia, Quarati, & Ricci, 1998; Haubold & Kumar, 2008; Lissia & Quarati, 2005). As we show in the next sections, a strong deviation from $q = 1$ is very unlikely for the BNN predictions, based on comparison with observations. Moreover, if $q$ deviates from the unity value, the lithium problem gets even worse.

# CHAPTER 2
# BIG BANG NUCLEOSYNTHESIS

## 2.1 Introduction

Big Bang Nucleosynthesis (BBN) is one of the most important evidences of the validity of the Standard Model in Cosmology. During the Big Bang the Universe evolved very rapidly and only the lightest nuclides (e.g., D, $^3$He, $^4$He, and $^7$Li) could be synthesized. The abundances of these nuclides are probes of the conditions of the Universe during the very early stages of its evolution. Historically, BBN was generally taken to be a three-parameter theory with results depending on the baryon density of the Universe, the neutron mean-life, and number of neutrino flavours (Reichl, 2009). By the early 1980s, primordial abundances of all four light elements synthesized in the big bang had been determined, and the concordance of the predicted abundances with the measured abundances was used both as a test of the big-bang framework and a means of constraining the baryon density.

## 2.2 Nuclear Equilibrium and Weak interaction freeze-out

In the beginning the universe was so hot that atomic nuclei could not form; space was filled with a mesh of protons, neutrons, leptons, photons and other short-lived particles. A proton and a neutron may collide and stick together to form a nucleus of deuterium, but at such high temperatures these clusters will be broken immediately by high-energy photons (photo-dissociation). During this time the weak interactions between neutrons, protons and leptons

$$\nu_e + n \leftrightarrow p + e, \tag{2.1}$$

$$e^+ + n \leftrightarrow p + \bar{\nu_e}, \tag{2.2}$$

$$n \leftrightarrow p + e^- + \bar{\nu_e}, \tag{2.3}$$

and the electromagnetic interaction between electrons and positrons

$$e^- + e^+ \leftrightarrow \gamma + \gamma, \tag{2.4}$$

keep all the particles in thermodynamic equilibrium. The weak interaction rate is defined by the Fermi Golden Rule as the number density of electrons multiplied by the weak interaction cross section, i.e.

$$\Gamma = n_e \sigma_{wk} = \frac{G_{wk}^2 (kT)^5}{\hbar}. \tag{2.5}$$

As the universe begins to expand it cools off and the weak process rates eventually become smaller than the expansion rate

$$H = \frac{1}{2t} = \sqrt{\frac{4\pi G g_* a_B}{3}} T^2 + c, \tag{2.6}$$

where c is a small constant. When this occurs some particle species can depart from thermodynamical equilibrium with the remaining plasma. At about $2 - 3$ MeV neutrinos undergo this process also known as *freezing out*. Soon after, at a temperature of

$$T_D = 0.7 MeV, \tag{2.7}$$

neutron-proton charged-current weak interactions also become too slow to maintain neutron-proton chemical equilibrium (Iocco, Mangano, Meile, Pisanti, & Serpico, 2009). It is now important to calculate the neutron-to-proton ratio because nearly all neutrons end up in $^4$He, allowing us to approximate the abundance of $^4$He. There are two considerations when calculating the number of neutrons, the number of neutrino families and the neutron lifetime $\tau_n$.

Figure 2.1 plots the different factors that determine the neutron-to-proton ratio as a function of time in seconds. Prior to the freeze-out at about 1 second, the relationship between the neutron lifetime and the weak coupling constant influences the weak reaction rates. The result on the neutron-to-proton ratio can be explained by the Boltzmann distribution as they are approximately in thermal equilibrium. According to the Boltzmann distribution (for more information see Chapter 3), the number ratio of neutrons to protons is

$$\frac{n_n}{n_p} = (\frac{m_n}{m_p})^{3/2} e^{-\Delta m / T_D}, \tag{2.8}$$

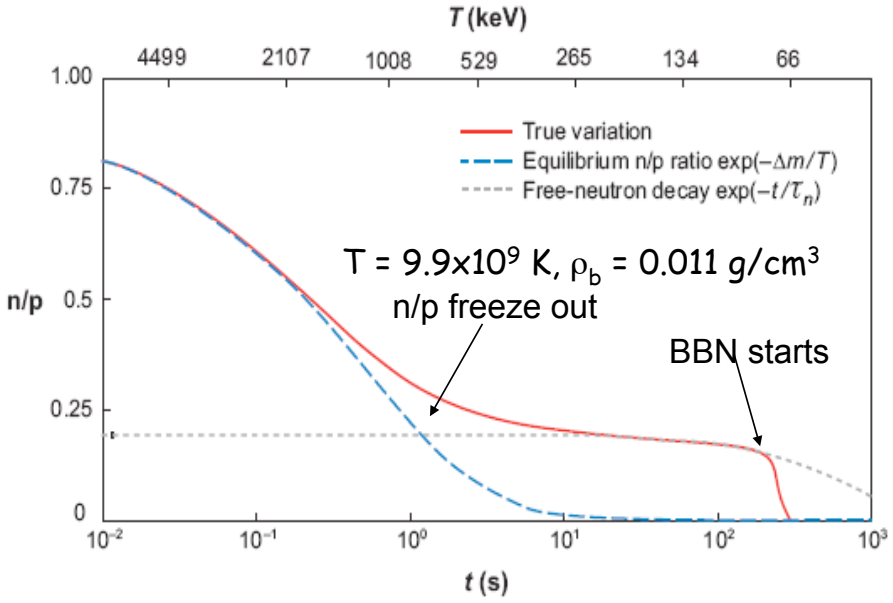


Figure 2.1: A plot of the neutron-to-proton ratio as a function of time. The dashed line represents the equilibrium ratio governed by the Boltzmann distribution whereas the dotted line takes into account the fact that free neutrons decay thus altering the ratio. The solid line is the result of both considerations.

where the neutron-proton mass difference

$$\Delta m = 1.29 MeV. \tag{2.9}$$

However, a free neutron is not stable and therefore we have to consider the effect of subsequent neutron decays between the interval t $\sim$ 1 s and t $\sim$ 200 s (weak freeze-out and start of nucleosynthesis). This modifies our previous equation to include the neutron decay rate resulting in

$$\frac{n_n}{n_p} = (\frac{m_n}{m_p})^{3/2} e^{-\Delta m/T_D} e^{-t/\tau_n}. \tag{2.10}$$

The neutron lifetime has been experimentally measured over the years and is shown in Figure 2.2. The x-axis is the baryon-to-photon ratio and the y-axis is the $^4$He abundance. We use the value of $\tau_n = 878.5 \pm 0.7 \pm 0.3$ s, according to the most recent experiements by A. Serebrov (2005), yielding a ratio of about one neutron to every seven protons.

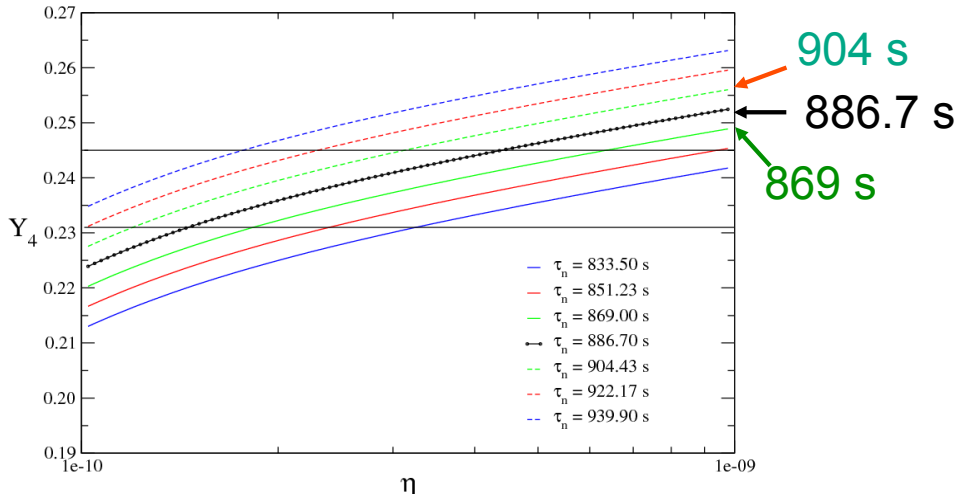


Figure 2.2: Free neutron lifetime calculations as a function of $\eta$, the baryon-to-photon ratio, and $Y_4$, the mass abundance of Helium 4. Both $\eta$ and $Y_4$ can be experimentally measured and where they intersect a value for the neutron lifetime is given.

The number of neutrino families is $N_\nu = 2.9840 \pm 0.0082$, as measured from the $Z_0$ width by LEP experiments at Collaboration (2006). In Figure 2.3, the big bang model is shown to be consistent with this measurement as it relates the observationally and theoretically predicted abundance of $^4$He (y-axis) to the number of neutrino families.

At this point, the binding energy (discussed later) of deuterium,

$$B_D \simeq 2.2MeV, \tag{2.11}$$

is greater than the photon temperature and thus one would expect that it is possible for deuterium to survive after forming from the process

$$n + p \rightarrow^2 H + \gamma. \tag{2.12}$$

This is not true due to the large photon-nucleon density ratio $\eta^{-1}$, which delays deuterium synthesis until the photo-dissociation process becomes ineffective, also known as the deuterium bottleneck. Once the high energy photons have become rare enough, i.e. sufficiently diluted by the expansion, it is possible for deuterium to remain and go on to combine with

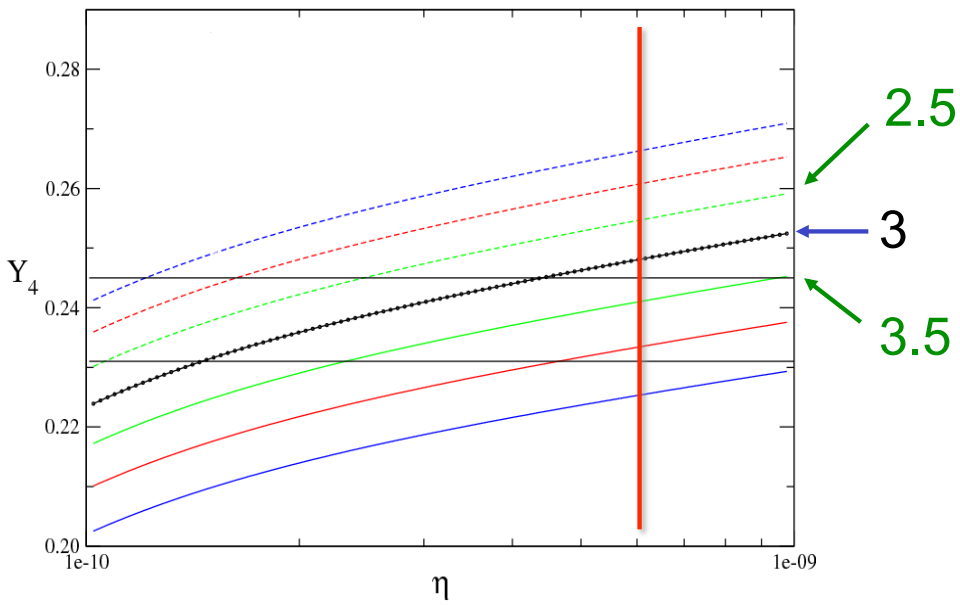


Figure 2.3: The number of neutrino families as a function of $\eta$, the baryon-to-photon ratio, and $Y_4$, the mass abundance of Helium 4. Both $\eta$ and $Y_4$ can be experimentally measured and where they intersect the number of neutrino families is given.

protons, neutrons and even other deuterium to form nuclei such as helium 3, helium 4, lithium and beryllium. This process of element-formation is known as "nucleosynthesis."

Eventually the universe is no longer hot and dense enough to maintain these processes but at some point other systems arise and continue where BBN left off. In fact evidence can be found in these systems that support the theory of BBN. Nuclear fusion of hydrogen in the core of stars produces helium but does not account for all of the helium. The most massive stars form the heavier elements up to iron, which has the highest nuclear binding energy of all elements and thus the most stable possible in a fusion reaction. To overcome this stability a large amount of energy, such as that of an exploding star (supernovae), is needed to produce elements heavier than iron. All of these processes involve the destruction of a lighter element in order to produce the heavier element. In fact, the lightest elements (deuterium, lithium and beryllium) are only destroyed within a star so they must have existed before the formation of stars.

However, there are reverse reactions, called fission, in which the heavier element dissociates into the more stable lighter element. The intricate web of fusion and fission

is known as the Nuclear Reaction Network and in the next section we will explore these processes in greater detail.

## 2.3 Nuclear Reaction Network

In a reaction network, nuclides of type j are created through reactions of type

$$k + l \rightarrow j + i \tag{2.13}$$

and destroyed through

$$j + m \rightarrow q + r. \tag{2.14}$$

These reactions can also be written in a more compact way such as k(l,j)i and j(m,q)r, which states target nucleus plus projectile yields ejectile plus produced nucleus. Common light particles such as protons, neutrons, deuterons, etc. are abbreviated when using this alternate method and are displayed in Table 2.1.

Table 2.1: Light Particle Abbreviations.

| Particle | Abbreviation |
|---|---|
| proton | p |
| neutron | n |
| deuteron | d |
| helium 4 | $\alpha$ |
| electron | $\beta$ |
| photon | $\gamma$ |

Depending on the reaction, the previously mentioned nuclides of type j absorb or emit a certain amount of energy when they are created or destroyed. This energy is known as the binding energy and is further defined in the next section.

### 2.3.1 Binding Energy

The strong interaction force between nucleons hold them together in order to form a stable nucleus. The energy required to break the nucleus into individual unbound components free of the strong force is known as the binding energy. The binding energy is defined by C. Bertulani (2007) as

$$B(Z, N) = \{Zm_p + Nm_n - m(Z, N)\}c^2, \tag{2.15}$$

where $m_p$ is the proton mass, $m_n$ the neutron mass, and $m(Z, N)$ the mass of the nucleus. This definition of binding energy is always positive due to the fact that the mass of the nucleus is smaller than the sum of the masses of its constituents, if measured separately.

In Figure 2.4 we show the binding energy per nucleon of each element. Out of the elements relevant to big bang nucleosynthesis, $^4$He has the largest binding energy and therefore the most stable during BBN. As a consequence, one would expect $^4$He to have the highest abundance out of the primordial elements. In order to determine this, all reactions must be considered, and in the next section we explore this topic.

### 2.3.2 BBN Reaction Network

Nuclear processes during the BBN proceed in a hot and low density plasma with a significant population of free neutrons, which expands and cools down very rapidly, resulting in peculiar "out of equilibrium" nucleosynthetic yields (Iocco et al., 2009). The low density of the plasma at the time of BBN is responsible for the suppression of three-body reactions and an enhanced effect of the Coulomb-barrier, which as a matter of fact inhibits any reaction with interacting nuclei charges

$$Z_1 Z_2 \geq 6. \tag{2.16}$$

The most efficient categories of reactions in BBN are therefore proton, neutron and deuterium captures, charge exchanges, and proton and neutron stripping (Iocco et al., 2009). The most important reactions in BBN are n-decay, p(n,$\gamma$)d, d(p,$\gamma$)$^3$He, d(d,n)$^3$He, d(d,p)t, $^3$He(n,p)t, t(d,n)$^4$He, $^3$He(d,p)$^4$He, $^3$He($\alpha,\gamma$)$^7$Be, t($\alpha,\gamma$)$^7$Li, $^7$Be(n,p)$^7$Li and $^7$Li(p,$\alpha$)$^4$He. These reactions are listed in Figure 2.5 and comprise the focus of our study.

## 2.4 Lithium Problem

In Figure 2.6 the x-axis is $\eta$, or the baryon to photon ratio, and on the y-axis is the abundance numbers relative to hydrogen. Therefore the plots labelled $^4$He, D, $^3$He and $^7$Li are the abundance numbers relative to hydrogen as a function of $\eta$ predicted by the BBN models. The vertical light blue line is the measured value of $\eta$ performed by WMAP, or the Wilkinson Microwave Anisotropy Probe. We should observe the abundance for each element where their plot intersects with the measured value of $\eta$. Our observations (solid

black boxes) do in fact coincide with the predicted values for $^4$He, D and $^3$He, however, the predicted value for $^7$Li is off by about a factor of four. Table 2.2 provides a side by side comparison of the BBN predicted abundance's to the observed abundance's.

Table 2.2: Predictions of the BBN (with $\eta_{WMAP} = 6.2\times10^{-10}$) with Maxwellian distributions compared with observations. All numbers have the same power of ten as in the last column.

| | Maxwell BBN | Observation |
|---|---|---|
| $^4$He/H | 0.249 | $0.2561 \pm 0.0108$ |
| D/H | 2.62 | $2.82^{+0.20}_{-0.19}(\times10^{-5})$ |
| $^3$He/H | 0.98 | $(1.1 \pm 0.2)(\times10^{-5})$ |
| $^7$Li/H | 4.39 | $(1.58 \pm 0.31)(\times10^{-10})$ |

The big bang model accurately reproduces many of our observations, but they are not in complete agreement. There have been many attempts at explaining the differences, such as, the predicted abundance is wrong due to poor cross section measurements, or perhaps our observation of the primordial lithium is wrong due to destruction processes (star destroyed, etc.). Over the years, attempts to solve this problem range from considering factors previously not thought of to increasing the accuracy of cross section measurements.

Electron screening has been considered by Wang, Bertulani, and Balantekin (2011). Our aim here is to see what role modifying the Boltzmann-distribution (see chapter 5) has on the abundances of the primordial elements. We go into detail in the following chapters.

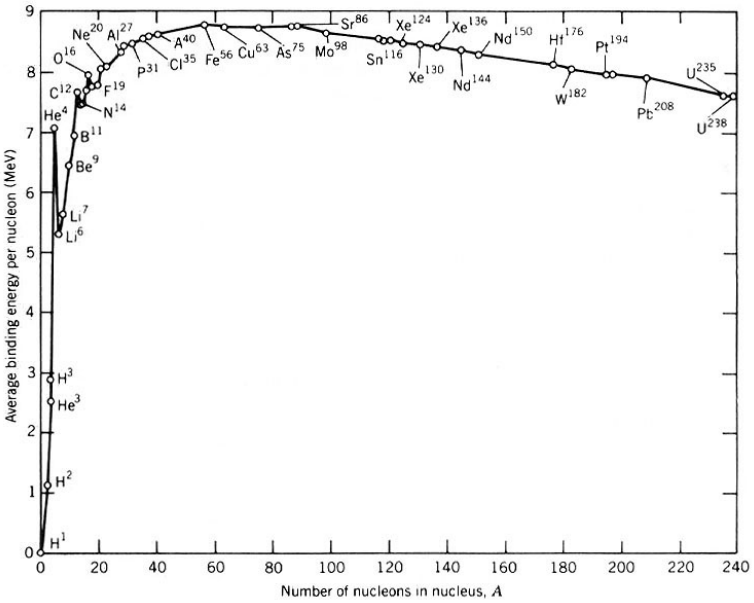


Figure 2.4: Binding Energy per nucleon, B/A, as a function of the mass number A. The picture is from Kraushaar (1984)

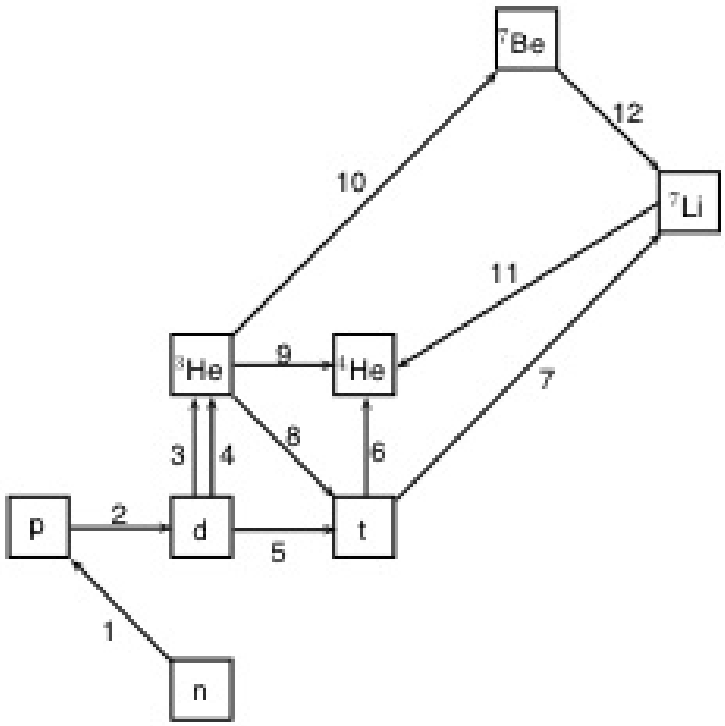


Figure 2.5: Nuclear Reaction Network for the most important reactions that occur during big bang nucleosynthesis. The picture is from Joakim Brorsson (2010).

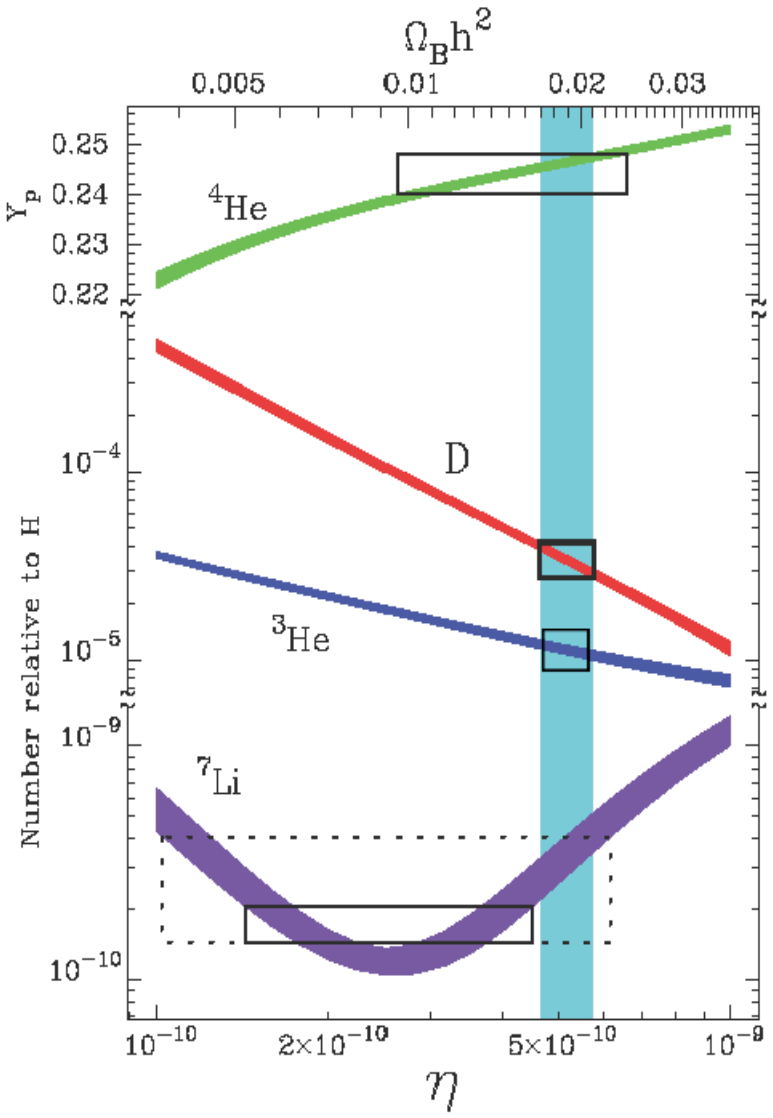


Figure 2.6: The predicted elemental abundance's of $^4$He, D, $^3$He and $^7$Li as a function of $\eta$, or the baryon-to-photon ratio. The vertical line is a measurement of $\eta$ performed by Komatsu (2011). Observations of the elemental abundance's are made (square boxes) and then compared to the predicted values provided by the measured value of $\eta$.

# CHAPTER 3
# MAXWELLIAN AND NON-MAXWELLIN DISTRIBUTIONS

Nuclear reaction rates in the BBN and in stelar evolution are strongly dependent of the particle velocity distributions. The fusion reaction rates for nuclear species 1 and 2 is given by $\langle \sigma v \rangle_{12}$, i.e., an average of the fusion cross section of $1+2$ with their relative velocity, described by a velocity distribution. It is thus worthwhile to study the modifications of the stellar reaction rates due to the modifications introduced by the non-extensive statistics.

## 3.1 Non-extensive Statistics

Statistical systems in equilibrium are described by the Boltzmann-Gibbs entropy,

$$\mathcal{S}_{BG} = -k_B \sum_i p_i \ln p_i, \tag{3.1}$$

where $k_B$ is the Boltzmann constant, and $p_i$ is the probability of the i-th microstate. For two independent systems $A$, $B$, the probability of the system $A + B$ being in a state $i + j$, with $i$ a microstate of $A$ and $j$ a microstate of $B$, is

$$p_{i+j}^{A+B} = p_i^A \cdot p_j^B. \tag{3.2}$$

Therefore, the Boltzmann-Gibbs entropy satisfies the relation

$$\mathcal{S}_{A+B} = \mathcal{S}_A + \mathcal{S}_B. \tag{3.3}$$

Thus, the entropy based on the Boltzmann-Gibbs statistic is an *extensive* quantity.

In the non-extensive statistics (Tsallis, 1988), one replaces the traditional entropy by the following one:

$$\mathcal{S}_q = k_B \frac{1 - \sum_i p_i^q}{q - 1}, \tag{3.4}$$

where $q$ is a real number. For $q = 1$, $\mathcal{S}_q = \mathcal{S}_{BG}$. Thus, the Tsallis statistics is a natural generalization of the Boltzmann-Gibbs entropy.

Now it follows that

$$\mathcal{S}_q(A+B) = \mathcal{S}_q(A) + \mathcal{S}_q(B) + \frac{(1-q)}{k_B}\mathcal{S}_q(A)\mathcal{S}_q(B). \tag{3.5}$$

The variable $q$ is a measure of the *non-extensivity*. Tsallis has shown that a formalism of statistical mechanics can be consistently developed in terms of this generalized entropy (Tsallis, 2009).

A consequence of the non- extensive formalism is that the distribution function which maximizes $S_q$ is non- Maxwellian (da Silva, Lima, & Santos, 2000; Muñoz, 2006; Silva, Plastino, & Lima, 1998). For $q = 1$, the Maxwell distribution function is reproduced. But for $q < 1$, high energy states are more probable than in the extensive case. On the other hand, for $q > 1$ high energy states are less probable than in the extensive case, and there is a cutoff beyond which no states exist.

## 3.2 Maxwellian Distribution

In stars, the thermonuclear reaction rate with a Maxwellian distribution is given by Fowler, Caughlan, and Zimmerman (1967)

$$\begin{aligned} R_{ij} &= \frac{N_i N_j}{1+\delta_{ij}}\langle\sigma v\rangle = \frac{N_i N_j}{1+\delta_{ij}}\left(\frac{8}{\pi\mu}\right)^{\frac{1}{2}}\left(\frac{1}{k_B T}\right)^{\frac{3}{2}} \\ &\times \int_0^\infty dE S(E)\exp\left[-\left(\frac{E}{k_B T} + 2\pi\eta(E)\right)\right], \end{aligned} \tag{3.6}$$

where $\sigma$ is the fusion cross section, $v$ is the relative velocity of the $ij$-pair, $N_i$ is the number of nuclei of species $i$, $\mu$ is the reduced mass of $i + j$, $T$ is the temperature, $S(E)$ is the astrophysical S-factor, and $\eta = Z_i Z_j e^2/\hbar v$ is the Sommerfeld parameter, with $Z_i$ the i-th nuclide charge and $E = \mu v^2/2$ is the relative energy of $i + j$.

The energy dependence of the reaction cross sections is usually expressed in terms of the equation

$$\sigma(E) = \frac{S(E)}{E}\exp\left[-2\pi\eta(E)\right]. \tag{3.7}$$

We write $2\pi\eta = b/\sqrt{E}$, where

$$b = 0.9898 Z_i Z_j \sqrt{A}\ \mathrm{MeV}^{1/2}, \tag{3.8}$$

where $A$ is the reduced mass in amu. The factor $1 + \delta_{ij}$ in the denominator of Eq. (3.6) corrects for the double-counting when $i = j$. The S-factor has a relatively weak dependence on the energy $E$, except when it is close to a resonance, where it is strongly peaked.

3.3 Non-Maxwellian Distribution

The non-extensive description of the Maxwell-Boltzmann distribution corresponds to the substitution $f(E) \to f_q(E)$, where (Tsallis, 2009)

$$\begin{aligned} f_q(E) &= \left[1 - \frac{q-1}{k_B T} E\right]^{\frac{1}{q-1}} \\ &\xrightarrow{q\to 1} \exp\left(-\frac{E}{k_B T}\right), \quad 0 < E < \infty. \end{aligned} \tag{3.9}$$

If $q - 1 < 0$, Eq. (3.9) is real for any value of $E \geq 0$. However, if $q - 1 > 0$, $f(E)$ is real only if the quantity in square brackets is positive. This means that

$$\begin{aligned} 0 \leq E \leq \frac{k_B T}{q-1}, \qquad & \text{if} \quad q \geq 1 \\ 0 \leq E, \qquad & \text{if} \quad q \leq 1. \end{aligned} \tag{3.10}$$

Thus, in the interval $0 < q < 1$ one has $0 < E < \infty$ and for $1 < q < \infty$ one has $0 < E < E_{\max} = k_B T/(q-1)$.

With this new statistics, the reaction rate becomes

$$R_{ij} = \frac{N_i N_j}{1 + \delta_{ij}} I_q, \tag{3.11}$$

and the rate integral, $I_q$, is given by

$$I_q = \int_0^{E_{max}} dE S(E) \mathcal{M}_q(E, T), \tag{3.12}$$

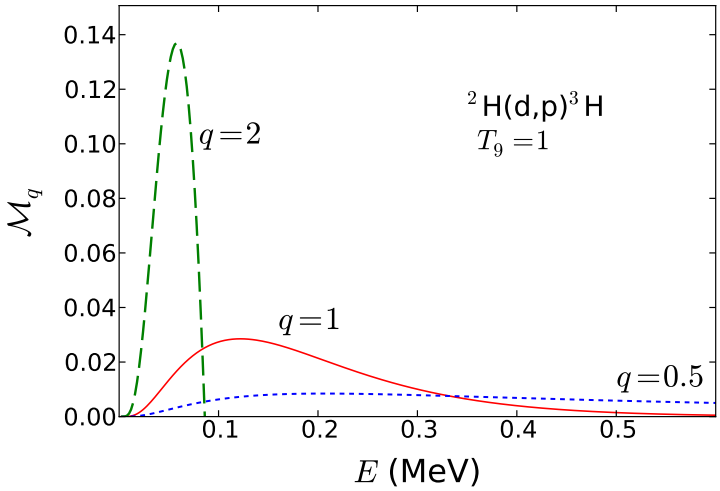


Figure 3.1: Modified Gamow distributions $\mathcal{M}_q(E,T)$ of deuterons relevant for the reaction $^2$H(d,p)$^3$H at $T_9 = 1$. The solid line, for $q = 1$, corresponds to the use of a Maxwell-Boltzmann distribution. Also shown are the results when using non-extensive distributions for $q = 0.5$ (dotted line) and $q = 2$ (dashed line).

where the "modified" Gamow energy distribution is

$$\begin{aligned}\mathcal{M}_q(E,T) &= \mathcal{A}(q,T)\left(1-\frac{q-1}{k_BT}E\right)^{\frac{1}{q-1}} e^{-b/\sqrt{E}} \\ &= \mathcal{A}(q,T)\left(1-\frac{q-1}{0.08617T_9}E\right)^{\frac{1}{q-1}} \\ &\times \exp\left[-0.9898Z_iZ_j\sqrt{\frac{A}{E}}\right] \end{aligned} \tag{3.13}$$

is the non-extensive Maxwell velocity distribution, $E_{max} = \infty$ for $0 < q < 1$ and $E_{\max} = k_BT/(1-q)$ for $1 < q < \infty$, and $E$ in MeV units. $\mathcal{A}(q,T)$ is a normalization constant which depends on the temperature and the non-extensive parameter $q$.

### 3.4 Non-Maxwellian distribution for relative velocities

It is worthwhile to notice that if the one-particle energy distribution is Maxwellian, it does not necessarily imply that the relative velocity distribution is also Maxwellian. Additional assumptions about correlations between particles are necessary to deduce that the relative-velocity distribution, which is the relevant quantity for rate calculations, is also Maxwellian. This has been discussed in details by Kaniadakis, Lissia, and Scarfone (2005);

Lissia and Quarati (2005); Tsallis (1988) where non-Maxwellian distributions, such as in Eq. (3.13), were shown to arise from non-extensive statistics.

Here we show that, if the non-Maxwellian particle velocity distribution is given by Eq. (3.9), then a two-particle relative can be modified to account for the center of mass recoil. Calling the kinetic energy of a particle $E_i$, this distribution is given by

$$f_q^{(i)} = \left(1 - \frac{q-1}{kT}E_i\right)^{\frac{1}{q-1}} \to \exp\left[-\left(\frac{E_i}{kT}\right)\right] \tag{3.14}$$

The two-particle energy distribution is $f_q^{(1)} f_q^{(2)}$. We now exponentiate the Tsallis distribution.

$$f_q^{(i)} = \exp\left\{\frac{1}{q-1}\left[\ln\left(1 - \frac{q-1}{kT}E_i\right)\right]\right\} \tag{3.15}$$

and the product $f_q^{(12)} = f_q^{(1)} f_q^{(2)}$ reduces to

$$f_q^{(12)} = \exp\left\{\frac{1}{q-1}\left[\ln\left(1 - \frac{q-1}{kT}E_1\right)\left(1 - \frac{q-1}{kT}E_2)\right)\right]\right\} \tag{3.16}$$

Since $E_i = m_i v_i^2/2$, and thus, $E_1 + E_2 = \mu v^2/2 + MV^2/2$, where $\mu$ is the reduced mass of the two particles, $M = m_1 + m_2$, $v$ is the relative velocity, and $V$ the center of mass velocity, the product inside the natural logarithm can be reduced to

$$\begin{aligned} &1 - \frac{1-q}{kT}\left(\frac{\mu v^2}{2} + \frac{MV^2}{2}\right) + \left(\frac{1-q}{kT}\right)^2 \frac{\mu v^2}{2}\frac{MV^2}{2} \\ &= \left(1 - \frac{1-q}{kT}\frac{\mu v^2}{2}\right)\left(1 - \frac{1-q}{kT}\frac{MV^2}{2}\right) \end{aligned} \tag{3.17}$$

Thus, the two-body distribution factorizes into a product of relative and center of mass parts

$$f_q^{(12)}(v, V, T) = f_q^{(rel)}(v, T) f_q^{(cm)}(V, T) \tag{3.18}$$

where

$$\begin{aligned} f_q^{(rel)}(v,T) &= \mathcal{A}_{rel}(q,T)\left(1-\frac{1-q}{kT}\frac{\mu v^2}{2}\right)^{\frac{1}{q-1}} \\ f_q^{(cm)}(V,T) &= \mathcal{A}_{cm}(q,T)\left(1-\frac{1-q}{kT}\frac{MV^2}{2}\right)^{\frac{1}{q-1}}, \end{aligned} \tag{3.19}$$

with the normalization constants obtained from the condition,

$$\int d^3v d^3V f_q^{(12)}(v,V,T) = 1. \tag{3.20}$$

Because the distribution factorizes, the unit normalization can be achieved for the relative and c.m. distributions separately. The distribution needed in the reaction rate formula is, therefore,

$$f_q(v,T) = \int d^3V f_q^{(12)}(v,V,T) = f_q^{(rel)}(v,T), \tag{3.21}$$

which attains the same form for as the absolute distribution.

In the limit $q \to 1$ the two-particle distribution reduces to a Gaussian, with the last term in the left-hand-side of Eq. (3.17) dropping out,

$$f_q^{(12)} = \mathcal{A}(q,T)\exp\left\{\left[-\left(\frac{\mu v^2/2 + MV^2/2}{kT}\right)\right]\right\}, \tag{3.22}$$

as expected.

### 3.5 Equilibrium with electrons, photons and neutrinos

One of the important questions regarding a plasma with particles (i.e., nuclei) described by the non-extensive statistics is how to generalize Fermi-Dirac, Bose-Einstein, and Tsallis statistics, to become more unified statistics with the distribution for the particles. This has been studied by Buyukkilic and Demirhan (2000), where it was shown that a similar non-extensive statistic for the distribution can be obtained for fermions and bosons is given by

$$n_q^{\pm}(E) = \frac{1}{\left[1-(q-1)\frac{(E-\mu)}{kT}\right]^{\frac{1}{q-1}} \pm 1}, \tag{3.23}$$

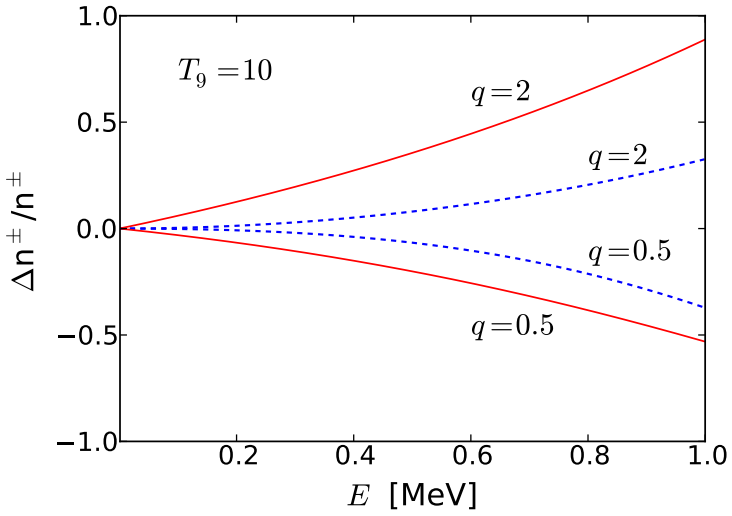


Figure 3.2: The relative difference ratio $(n_q^{\pm} - n^{\pm})/n^{\pm}$ between non-extensive, $n_q$, and extensive, $n = n_{q\to 1}$, statistics. Solid curves are for Fermi-Dirac statistics, $n^+$, and dashed curves are for Bose-Einstein statistics, $n^-$. For both distributions, we use $\mu = 0$. Results are shown for $q = 2$ and $q = 0.5$, with $T_9 = 10$.

where $\mu$ is the chemical potential. This reproduces the Fermi distribution, $n^+$, for $q \to 1$ and the Bose-Einstein distribution for photons, $n^-$, for $\mu = 0$ and $q \to 1$. Planck's law for the distribution of radiation is obtained by multiplying $n^-$ in Eq. (3.23) (with $\mu = 0$) by $\hbar\omega^2/(4\pi^2c^2)$, where $E = \hbar\omega$. The number density of electrons can be obtained from $n^+$ in Eq. (3.23) with the proper phase-factors depending if the electrons are non-relativistic or relativistic. Normalization factors $\mathcal{A}^{\pm}(q, T)$ also need to be introduced, as before.

The electron density during the early universe varies strongly with the temperature. At $T_9 = 10$ the electron density is about $10^{32}/\text{cm}^3$, much larger than the electron number density at the center of the sun, $n_e^{sun} \sim 10^{26}/\text{cm}^3$. The large electron density is due to the $e^+e^-$ production by the abundant photons during the BBN. However, the large electron densities do not influence the nuclear reactions during the BBN. In fact, the enhancement of the nuclear reaction rates due to electron screening were shown to be very small (Wang et al., 2011). The electron Fermi energy for these densities are also much smaller than $kT$ for the energy relevant for BBN, so that one can also use $\mu = 0$ in Eq. (3.23) for $n^+$.

In Figure 3.2 we plot the the relative difference ratio $(n_q^{\pm} - n^{\pm})/n^{\pm}$ between non-extensive, $n_q$, and extensive, $n = n_{q\to 1}$, statistics. For both distributions, we use $\mu = 0$.

The solid curves are for Fermi-Dirac (FD) statistics, $n^+$, and dashed curves are for Bose-Einstein (BE) statistics, $n^-$. We show results for $q = 2$ and $q = 0.5$, with $T_9 = 10$. One sees that the non-extensive distributions are enhanced for $q > 1$ and suppressed for $q < 1$, as compared to the respective FD and BE quantum distributions. The deviations for the FD and BE statistics also grow larger with the energy. For example, the non-extensive electron distribution is roughly a factor 2 larger than the usual FD distribution at $E_e = 1$ MeV, at $T_9 = 10$.

While we don't obtain numerical results with modified Fermi-Dirac and Bose-Einstein distributions here, it can be expected that these generalizations will have a strong influence on the freezout temperature and the neutron to proton, $n/p$, ratio. A numerical study of this problem may be presented in another paper. The freezout temperature, occurs when the rate, $\Gamma \sim \langle \sigma v \rangle$, for weak reaction $\nu_e + n \rightarrow p + e^-$ becomes slower than the expansion rate of the Universe. Because during the BBN the densities of all particles, including neutrinos, are low compared to $kT$, the chemical potential $\mu$ can be set to zero in the calculation of all reaction rates. The adoption of non-extensive quantum distributions such as in Eq. (3.23) will lead to the same powers of the temperature as those predicted by the FD distribution and the Bose-Einstein distribution. For example, Planck law for the total blackbody is $U \propto T^4$, being form invariant with respect to non-extensivity entropic index $q$ which determines the the degree of non-extensivity (Sokmen, Buyukkilic, & Demirhan, 2002). This result means that the weak decay reaction rates do not depend on the non-extensive parameter $q$. The freezout temperature and $n/p$ ratio remain the same as before.

More detailed studies have indicated that Planck's law of blackbody radiation and other thermodynamical quantities arising from non-extensive quantum statistics can yield different powers of temperature than for the non-extensive case (Aragao-Rego, 2003; Chamati, Djankova, & Tonchev, 2003; Nauenberg, 2003; Tsallis, 2004). If that is the case, then a study of the influence of non-extensive statistics on the weak-decay rates and electromagnetic processes during BBN is worth pursuing.

### 3.6 Thermodynamical equilibrium

The physical appeal for non-extensivity is the role of long-range interactions, which also implies non-equilibrium. Accepting non-extensive entropy means abandoning the most important concept of thermodynamics, namely the tendency of any system to reach equilibrium. This also means that the concept of non-extensivity means renouncing the second law of thermodynamics altogether!

The comments above, which seem to be shared by part of the community [see, e.g., Bouchet, Dauxois, and Ruffo (2006); Damian H. Zanette (2003); Dauxois (2007); Nauenberg (2003); Touchette (2013); Zanette and Montemurro (2004)], are worrisome when one has to consider a medium composed of particles obeying classical and quantum statistics. It is not clear for example if the non-extensive parameter $q$ has to be the same for all particle distributions, both classical and quantum. Even worse is the possibility that the temperatures are not the same for the different particle systems in the plasma.

In the present work, we will avoid a longer discussion on the validity of the Tsallis statistics for a plasma such as that existing during the BBN. We will only consider the effect of its use for calculating nuclear reaction rates in the plasma, assuming that it can be described by a classical distribution of velocities. This study will allow us to constrain the non-extensive parameter $q$ based on a comparison with observations.

# CHAPTER 4
# REACTION RATES DURING BIG BANG NUCLEOSYNTHESIS

Based on the abundant literature on non-extensive statistics [see, e.g., Coraddu (1999); Degl'Innocenti et al. (1998); Haubold and Kumar (2008); Lissia and Quarati (2005); Tsallis (1988)], we do not expect that the non-extensive parameter $q$ differs appreciably from the unity value. However, in order to study the influence of a non-Maxwellian distribution on BBN we will explore values of $q$ rather different than the unity, namely, $q = 0.5$ and $q = 2$. This will allow us to pursue a better understanding of the nature of the physics involved in the departure from the BG statistics. In Figure 3.1 we plot the Gamow energy distributions of deuterons relevant for the reaction $^2$H(d,p)$^3$H at $T_9 = 1$. The solid line, for $q = 1$, corresponds to the use of the Maxwell-Boltzmann distribution. Also shown are results for non-extensive distributions for $q = 0.5$ (dotted line) and $q = 2$ (dashed line). One observes that for $q < 1$, higher kinetic energies are more accessible than in the extensive case ($q = 1$). For $q > 1$ high energies are less probable than in the extensive case, and there is a cutoff beyond which no kinetic energy is reached. In the example shown in the Figure for $q = 2$, the cutoff occurs at 0.086 MeV, or 86 keV.

We will explore the modifications of the BBN elemental abundances due to a variation of the non-extensive statistics parameter $q$. We will express our reaction rates in the form $N_A\langle\sigma v\rangle$ (in units of cm$^3$ mol$^{-1}$ s$^{-1}$), where $N_A$ is the Avogadro number and $\langle\sigma v\rangle$ involves the integral in Eq. (3.6) with the Maxwell distribution $f(E)$ replaced by Eq. (3.9). First we show how the reaction rates are modified for $q \neq 1$.

In Figure 4.1 we show the S-factor for the reaction $^2$H(d,p)$^3$H as a function of the relative energy $E$. Also shown is the dependence on $T_9$ (temperature in units of $10^9$ K) for the effective Gamow energy

$$E = E_0 = 0.122(Z_i^2 Z_j^2 A)^{1/3} T_9^{2/3} \text{ MeV}, \tag{4.1}$$

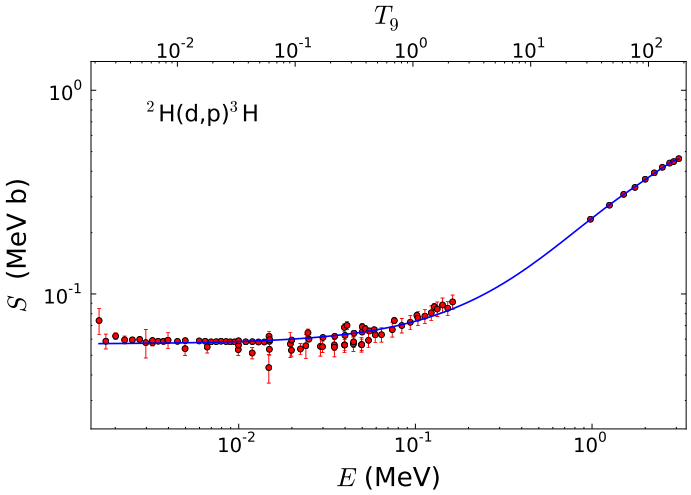


Figure 4.1: S-factor for the reaction $^2$H(d,p)$^3$H as a function of the relative energy $E$ and of the temperature $T_9$. The data are from Bosch and Hale (1992); Brown and Jarmie (1990); Krauss et al. (1987); Schulte et al. (1972); U. Greife (1995). The solid curve is a polynomial fit to the experimental data.

where $A$ is the reduced mass in amu. The data are from Bosch and Hale (1992); Brown and Jarmie (1990); Krauss et al. (1987); Schulte et al. (1972); U. Greife (1995) and the solid curve is a chi-square polynomial function fit to the data.

Using the chi-square polynomial fit obtained to fit the data presented in Figure 4.1, we show in Figure 4.2 the reaction rates for $^2$H(d,p)$^3$H as a function of the temperature $T_9$ for two different values of the non-extensive parameter $q$. The integrals in equation (3.12) are performed numerically. For charge particles, a good accuracy (witihin 0.1%) is reached using the integration limits between $E_0 - 5\Delta E$ and $E_0 + 5\Delta E$, where $\Delta E$ is given by Eq. (4.2) below. The rates are expressed in terms of the natural logarithm of $N_A\langle\sigma v\rangle$ (in units of cm$^3$ mol$^{-1}$ s$^{-1}$). The solid curve corresponds to the usual Maxwell-Boltzmann distribution, i.e., $q = 1$. The dashed and dotted curves are obtained for $q = 2$ and $q = 0.5$, respectively. In both cases, we see deviations from the Maxwellian rate. For $q > 1$ the deviations are rather large and the tendency is an overall suppression of the reaction rates, specially at low temperatures. This effect arises from the non-Maxwellian energy cutoff which for this reaction occurs at $0.086T_9$ MeV and which prevents a great number of reactions to occur at higher energies.

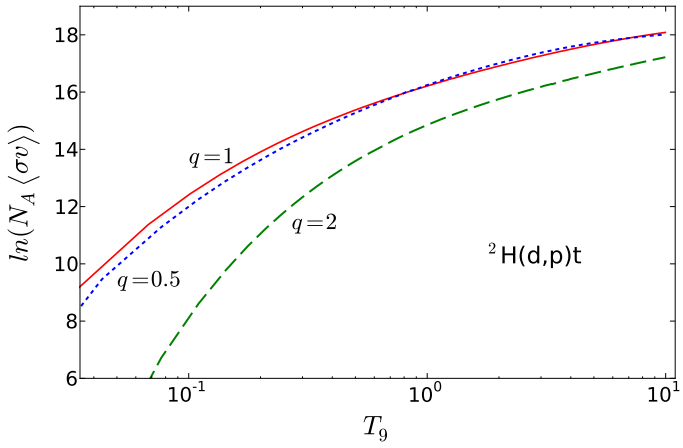


Figure 4.2: Reaction rates for $^2$H(d,p)$^3$H as a function of the temperature $T_9$ for different values of the non-extensive parameter $q$. The rates are given in terms of the natural logarithm of $N_A\langle\sigma v\rangle$ (in units of cm$^3$ mol$^{-1}$ s$^{-1}$). Results with the use of non-extensive distributions for $q = 0.5$ (dotted line) and $q = 2$ (dashed line) are shown.

For $q < 1$ the nearly similar result as with the Maxwell-Boltzmann distribution is due to a competition between suppression in reaction rates at low energies and their enhancement at high energies. The relevant range of energies is set by the Gamow energy which for a Maxwellian distribution is given by Eq. (4.1) and by the energy window,

$$\Delta E = 0.2368(Z_i^2 Z_j^2 A)^{1/6} T_9^{5/6} \text{ MeV}, \tag{4.2}$$

which for the reaction $^2$H(d,p)$^3$H amounts to $0.2368T_9^{5/6}$ MeV. This explains why, at $T_9 = 1$, the range of relevant energies for the calculation of the reaction rate is shown by the solid curve in Figure 3.1. For $q < 1$ the Gamow window $\Delta E$ is larger and there is as much a contribution from the suppression of reaction rates at low energies compared to the Maxwell-Boltzmann distribution, as there is a corresponding enhancement at higher energies. This explains the nearly equal results shown in Figure 4.2 for $q = 1$ and $q < 1$. This finding applies to all charged particle reaction rates, except for those when the S-factor has a strong dependence on energy at, and around, $E = E_0$. But no such behavior exists for the most

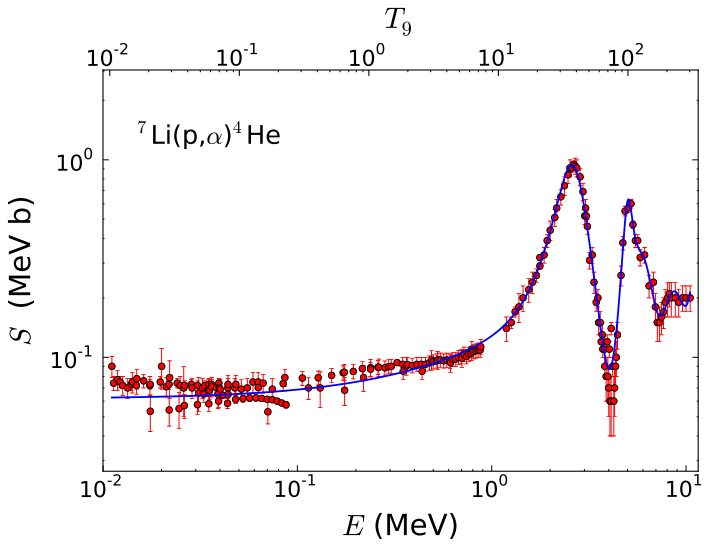


Figure 4.3: S-factor for the reaction $^7$Li(p,$\alpha$)$^4$He as a function of the relative energy $E$ and of $T_9$. The data are from Cassagnou et al. (1962, 1963); Fiedler and Kunze (1967); G. S. Mani (1964); H. Spinka and Winkler (1971); J.M. Freeman (1958); Lerner and Marion (1969); Rolfs and Kavanagh (1986); S. Engstler (1992a, 1992b); Werby (1973). The solid curve is a chi-square function fit to the data using a sum of polynomials plus Breit-Wigner functions.

important charged induced reactions in the BBN (neutron-induced reactions will be discussed separately).

The findings described above for the reaction $^2$H(d,p)$^3$H are not specific but apply to all charged particles of relevance to the BBN. We demonstrate this with one more example: the $^7$Li(p,$\alpha$)$^4$He reaction, responsible for $^7$Li destruction. In Figure 4.3 we show the S-factor for this reaction as a function of the relative energy $E$. One sees prominent resonances at higher energies. Also shown in the Figure is the dependence of the reaction on $T_9$. The data are from Cassagnou et al. (1962, 1963); Fiedler and Kunze (1967); G. S. Mani (1964); H. Spinka and Winkler (1971); J.M. Freeman (1958); Lerner and Marion (1969); Rolfs and Kavanagh (1986); S. Engstler (1992a, 1992b); Werby (1973) and the solid curve is a chi-square function fit to the data using a sum of polynomials plus Breit-Wigner functions.

Using the chi-square function fit obtained to fit the data presented in Figure 4.3, we show in Figure 4.4 the reaction rates for $^7$Li(p,$\alpha$)$^4$He as a function of the temperature $T_9$ for two different values of the non-extensive parameter $q$. The rates are given in terms of

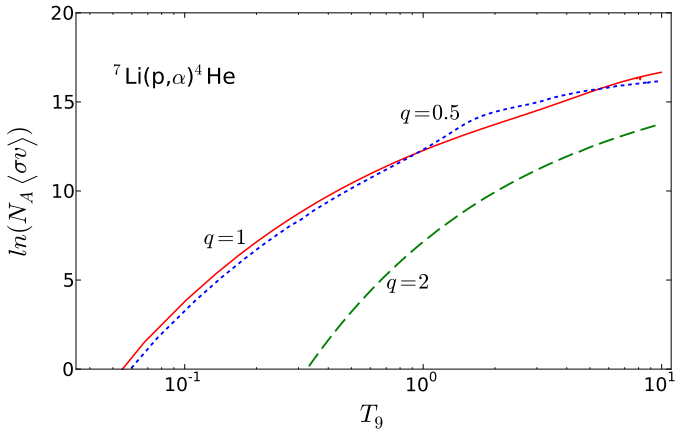


Figure 4.4: Reaction rates for $^7$Li(p,$\alpha$)$^4$He as a function of the temperature $T_9$ for two different values of the non-extensive parameter $q$. The rates are given in terms of the natural logarithm of $N_A\langle\sigma v\rangle$ (in units of cm$^3$ mol$^{-1}$ s$^{-1}$). Results with the use of non-extensive distributions for $q = 0.5$ (dotted line) and $q = 2$ (dashed line) are shown.

the natural logarithm of $N_A\langle\sigma v\rangle$ (in units of cm$^3$ mol$^{-1}$ s$^{-1}$). The solid curve corresponds to the usual Maxwell-Boltzmann distribution, i.e., $q = 1$. The dashed and dotted curves are obtained for $q = 2$ and $q = 0.5$, respectively. As with the reaction presented in Figure 4.2, in both cases we see deviations from the Maxwellian rate. But, as before, for $q = 2$ the deviations are larger and the tendency is a strong suppression of the reaction rates as the temperature decreases. It is interesting to note that the non-Maxwellian rates for $q = 0.5$ are more sensitive to the resonances than for $q > 1$. This is because, as seen in Figure 3.1, for $q < 1$ the velocity distribution is spread to considerably larger values of energies, being therefore more sensitive to the location of high energy resonances.

We now turn to neutron induced reactions, which are only a few cases of high relevance for the BBN, notably the p(n,$\gamma$)d, $^3$He(n,p)t, and $^7$Be(n,p)$^7$Li reactions. For neutron induced reactions, the cross section at low energies is usually proportional to $1/v$, where $v = \sqrt{2mE}/\hbar$ is the neutron velocity. Thus, it is sometimes appropriate to rewrite Eq. (3.7) as

$$\sigma(E) = \frac{S(E)}{E} = \frac{R(E)}{\sqrt{E}} \tag{4.3}$$

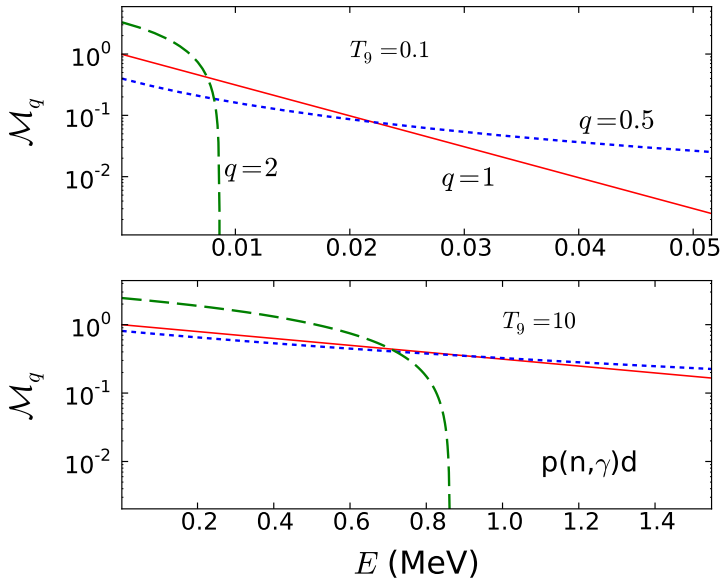


Figure 4.5: Spectral function $\mathcal{M}_q(E,T)$ for protons and neutrons relevant for the reaction p(n,$\gamma$)d at $T_9 = 0.1$ (upper panel) and $T_9 = 10$ (lower panel). The solid line, for $q = 1$, corresponds to the usual Boltzmann distribution. Also shown are non-extensive distributions for $q = 0.5$ (dotted line) and $q = 2$ (dashed line).

where $R(E)$ is a slowly varying function of energy similar to an $S$-factor. The distribution function within the reaction rate integral (3.12) is also rewritten as

$$\mathcal{M}_q(E,T) \;\; = \mathcal{A}(q,T) f_q(E) = \;\; \mathcal{A}(q,T) \left(1 - \frac{q-1}{k_B T} E\right)^{\frac{1}{q-1}} . \tag{4.4}$$

The absence of the tunneling factor $\exp(-b/\sqrt{E})$ in Eq. (4.4) inhibts the dependence of the reaction rates on the non-extensive parameter $q$.

In Figure 4.5 we plot the kinetic energy distributions of nucleons relevant for the reaction p(n,$\gamma$)d at $T_9 = 0.1$ (upper panel) and $T_9 = 10$ (lower panel). The solid line, for $q = 1$, corresponds to the usual Boltzmann distribution. Also shown are results for the non-extensive distributions for $q = 0.5$ (dotted line) and $q = 2$ (dashed line). One observes that, as for the charged particles case, with $q < 1$ higher kinetic energies are more probable than in the extensive case ($q = 1$). With $q > 1$ high energies are less accessible than in the extensive case, and there is a cutoff beyond which no kinetic energy is reached. A noticeable

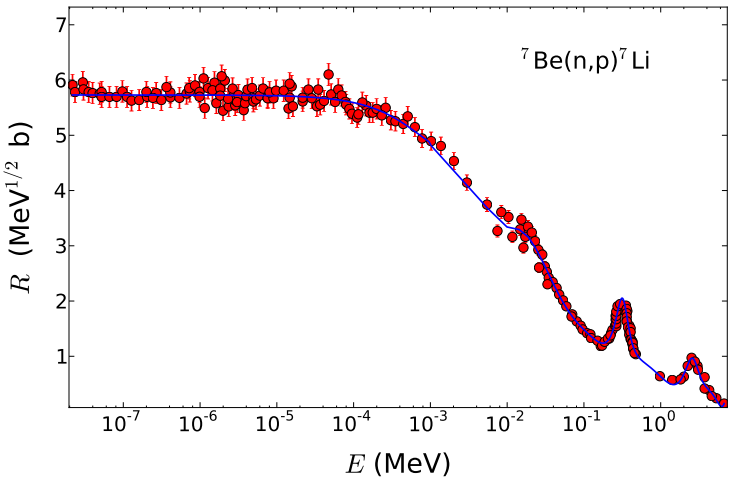


Figure 4.6: The energy dependence of $R(E) = S(E)\sqrt{E}$ for the reaction $^7$Be(n,p)$^7$Li. is shown in Figure 4.6. The experimental data were collected from Borchers and Poppe (1963); Gibbons and Macklin (1959); Koehler (1988); Poppe et al. (1976); Sekharan (1976). The solid curve is a function fit to the experimental data using a set of polynomials and Breit-Wigner functions.

difference form the case of charged particles is the absence of the Coulomb barrier and a correspondingly lack of suppression of the reaction rates at low energies. As the temperature increases, the relative difference between the Maxwell-Boltzmann and the non-Maxwellian distributions decrease appreciably. This will lead to a rather distinctive pattern of the reaction rates for charged compared to neutron induced reactions.

For neutron-induced reactions, a good accuracy (within 0.1%) for the numerical calculation of the reaction rates with Eq. (3.12) is reached using the integration limits between $E = 0$ and $E = 20k_BT$. As an example we will now consider the reaction $^7$Be(n,p)$^7$Li. The energy dependence of $R(E) = S(E)\sqrt{E}$ for this reaction is shown in Figure 4.6. The experimental data were collected from Borchers and Poppe (1963); Gibbons and Macklin (1959); Koehler (1988); Poppe et al. (1976); Sekharan (1976).

Using the chi-square fit with a sum of polynomials and Breit-Wigners obtained to reproduce the data in Figure 4.6, we show in Figure 4.7 the reaction rates for $^7$Be(n,p)$^7$Li as a function of the temperature $T_9$ for different values of the non-extensive parameter $q$. The rates are given in terms of the natural logarithm of $N_A\langle\sigma v\rangle$ (in units of cm$^3$ mol$^{-1}$ s$^{-1}$).

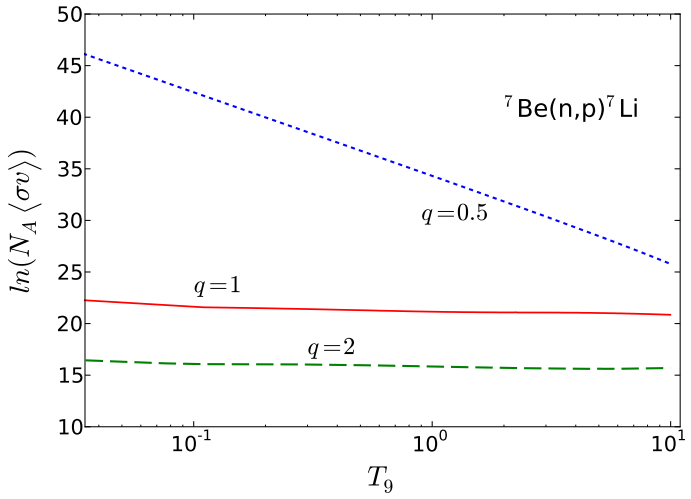


Figure 4.7: Reaction rates for $^7$Be(n,p)$^7$Li as a function of the temperature $T_9$ for two different values of the non-extensive parameter $q$. The rates are given in terms of the logarithm of $N_A\langle\sigma v\rangle$ (in units of cm$^3$ mol$^{-1}$ s$^{-1}$). Results with the use of non-extensive distributions for $q = 0.5$ (dotted line) and $q = 2$ (dashed line) are shown.

The solid curve corresponds to the usual Boltzmann distribution, i.e., $q = 1$. The dashed and dotted curves are obtained for $q = 2$ and $q = 0.5$, respectively. In contrast to reactions induced by charged particles, we now see strong deviations from the Maxwellian rate both for $q > 1$ and $q < 1$. For $q < 1$ the deviations are larger at small temperatures and decrease as the energy increase, tending asymptotically to the Maxwellian rate at large temperatures. This behavior can be understood from Figure 4.5 [for $^7$Be(n,p)$^7$Li the results are nearly the same as in Fig. 4.5]. At small temperatures, e.g. $T_9 = 0.1$, the distribution for $q = 0.5$ is strongly enhanced at large energies and the tendency is that the reaction rates increase at low temperatures. This enhancement disappears as the temperature increase (lower panel of Figure 4.5). For $q = 2$ the reaction rate is suppressed, although not as much as for the charged-induced reactions, the reason being due a compensation by an increase because of normalization at low energies.

Having discussed the dependence of the reaction rates on the non-extensive parameter $q$ for a few standard reactions, we now consider the implications of the non-extensive statistics to the predictions of the BBN. It is clear from the results presented above that an appreciable impact on the abundances of light elements will arise.

# CHAPTER 5
# BBN WITH NON-EXTENSIVE STATISTICS

The BBN is sensitive to certain parameters, including the baryon-to-photon ratio, number of neutrino families, and the neutron decay lifetime. We use the values $\eta = 6.19 \times 10^{-10}$, $N_\nu = 3$, and $\tau_n = 878.5$ s for the baryon-photon ratio, number of neutrino families, and neutron-day lifetime, respectively. Our BBN abundances were calculated with a modified version of the standard BBN code derived from Kawano (1988, 1992); Wagoner, Fowler, and Hoyle (1967).

Although BBN nucleosynthesis can involve reactions up to the CNO cycle (Coc, Goriely, Xu, Saimpert, & Vangioni, 2012), the most important reactions which can significantly affect the predictions of the abundances of the light elements ($^4$He, D, $^3$He, $^7$Li) are n-decay, p(n,$\gamma$)d, d(p,$\gamma$)$^3$He, d(d,n)$^3$He, d(d,p)t, $^3$He(n,p)t, t(d,n)$^4$He, $^3$He(d,p)$^4$He, $^3$He($\alpha,\gamma$)$^7$Be, t($\alpha,\gamma$)$^7$Li, $^7$Be(n,p)$^7$Li and $^7$Li(p,$\alpha$)$^4$He. Except for these reactions, we have used the reaction rates needed for the remaining reactions from a compilation by NACRE (Angulo, 1999) and that reported in Descouvemont, Adahchour, Angulo, Coc, and Vangioni-Flam (2004). For the 11 reactions mentioned above, we have collected data from Angulo (1999); Descouvemont et al. (2004); Smith, Kawano, and Malaney (1993), and references mentioned therein [data for n(p,$\gamma$)d reaction was taken from the on-line ENDF database (*http://www.nndc.bnl.gov*, n.d.) - see also Ando, Cyburt, Hong, and Hyun (2006); Cyburt (2004)], fitted the S-factors with a sum of polynomials and Breit-Wigner functions and calculated the reaction rates for Maxwellian and non-Maxwellian distributions.

In Figure 5.1 we show the calculated deuterium abundance. The solid curve is the result with the standard Maxwell distributions for the reaction rates. Using the non-extensive distributions yields the dotted line for $q = 0.5$ and the dashed line for $q = 2$. It is interesting to observe that the deuterium abundances are only moderately modified due to the use of the non-extensive statistics for $q = 0.5$. Up to temperatures of the order of $T_9 = 1$, the abundance for D/H tends to agree for the extensive and non-extensive statistics. This is due to the fact that any deuterium that is formed is immediately destroyed (a situation

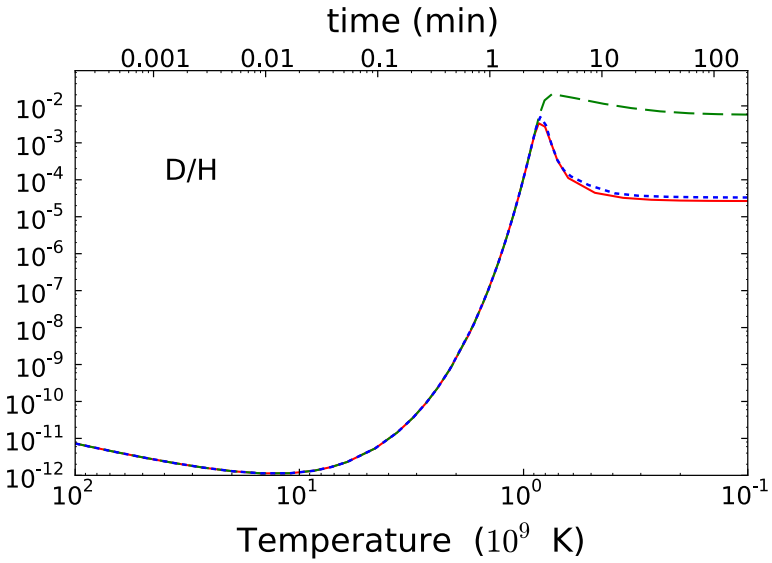


Figure 5.1: Deuterium abundance. The solid curve is the result obtained with the standard Maxwell distributions for the reaction rates. Results with the use of non-extensive distributions for $q = 0.5$ (dotted line) and $q = 2$ (dashed line) are shown.

known as the deuterium bottleneck). But, as the temperature decreases, the reaction rates for the p(n,$\gamma$)d reaction are considerably enhanced for $q = 2$ (see Figure 4.5), and perhaps more importantly, they are strongly suppressed for all other reactions involving deuterium destruction, as clearly seen in Figure 4.2. This creates an unexpected over abundance of deuterons for the non-extensive statistics with $q = 2$. The deuterium, a very fragile isotope, is easily destroyed after the BBN and astrated. Its primordial abundance is determined from observations of interstellar clouds at high redshift, on the line of sight of distant quasars. These observations are scarce but allow to set an average value of D/H $= 2.82^{+0.20}_{-0.19} \times 10^{-5}$ (Pettini, 2008). The predictions for the D/H ratio with the $q = 2$ statistics (D/H $= 5.70 \times 10^{-3}$) is about a factor 200 larger than those from the standard BBN model, clearly in disagreement with the observation.

A much more stringent constraint for elemental abundances is given by $^4$He, which observations set at about $^4$He/H $\equiv Y_p = 0.2561 \pm 0.0108$ (Aver, Olive, & Skillman, 2010; Boesgaard & Steigman, 1985; Izotov & Thuan, 2010). The $^4$He abundance generated from our BBN calculation is plotted in Figure 5.2. The solid curve is the result obtained with the standard Maxwell distribution for the reaction rates. Using the non-extensive distributions

Table 5.1: Predictions of the BBN (with $\eta_{WMAP} = 6.2 \times 10^{-10}$) with Maxwellian and non-Maxwellian distributions compared with observations. All numbers have the same power of ten as in the last column.

| | Maxwell BBN | Non-Max. $q = 0.5$ | Non-Max. $q = 2$ | Observation |
|---|---|---|---|---|
| $^4$He/H | 0.249 | 0.243 | 0.141 | $0.2561 \pm 0.0108$ |
| D/H | 2.62 | 3.31 | 570.0 | $2.82^{+0.20}_{-0.19}(\times 10^{-5})$ |
| $^3$He/H | 0.98 | 0.091 | 69.1 | $(1.1 \pm 0.2)(\times 10^{-5})$ |
| $^7$Li/H | 4.39 | 6.89 | 356.0 | $(1.58 \pm 0.31)(\times 10^{-10})$ |

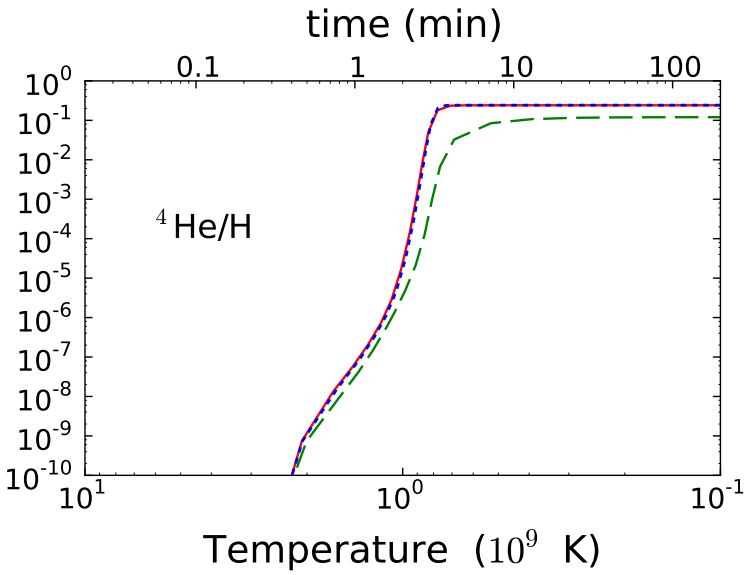


Figure 5.2: $^4$He abundance. The solid curve is the result obtained with the standard Maxwell distributions for the reaction rates. Results with the use of non-extensive distributions for $q = 0.5$ (dotted line) and $q = 2$ (dashed line) are also shown.

yields the dotted line for $q = 0.5$ and the dashed line for $q = 2$. Again, the predicted abundances for $q = 2$ deviate substantially from standard BBN results. This time only about half of $^4$He is produced with the use of a non-extensive statistics with $q = 2$. The reason for this is the suppression of the reaction rates for formation of $^4$He with $q = 2$ through the charged particle reactions t(d,n)$^4$He, $^3$He(d,p)$^4$He.

A strong impact of using non-extensive statistics for both $q = 0.5$ and $q = 2$ values of the non-extensive parameter is seen in Figure 5.3 for the $^3$He abundance. While for $q = 2$ there is an overshooting in the production of $^3$He, for $q = 0.5$ one finds a smaller value than the one predicted by the standard BBN. This is due to the distinct results for the destruction

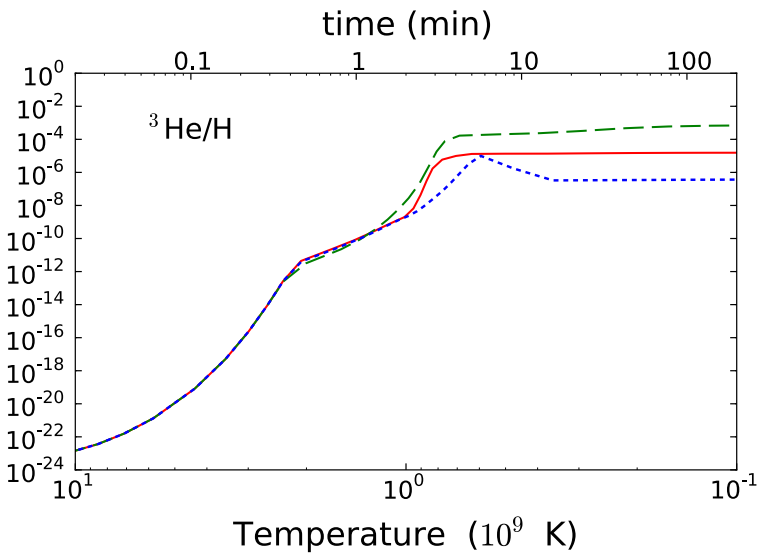


Figure 5.3: $^{3}$He abundance. The solid curve is the result obtained with the standard Maxwell distributions for the reaction rates. Results with the use of non-extensive distributions for $q = 0.5$ (dotted line) and $q = 2$ (dashed line) are also shown.

of $^{3}$He through the reaction $^{3}$He(n,p)t, which is enhanced for $q = 0.5$ and suppressed for $q = 2$, in the same way as it happens for the reaction $^{7}$Be(n,p)$^{7}$Li, shown in Figure 4.6. $^{3}$He is both produced and destroyed in stars and its abundance is still subject to large uncertainties, $^{3}\mathrm{He/H} = (1.1 \pm 0.2) \times 10^{-5}$ (Bania, Rood, & Balser, 2002; Vangioni-Flam, Olive, Fields, & Casse, 2003).

Non-extensive statistics for both $q = 0.5$ and $q = 2$ values also alter substantially the $^{7}$Li abundance, as shown in Figure 5.4. For both values of the non-extensive parameter $q = 2$, and $q = 0.5$, there is an overshooting in the production of $^{7}$Li. The increase in the $^{7}$Li abundance is more accentuated for $q = 2$. The lithium problem is associated with a smaller value of the observed $^{7}$Li abundance as compared the predictions of BBN. There has been many attempts to solve this problem by testing all kinds of modifications of the parameters of the BBN or the physics behind it [a sample of this literature is found in Boyd, Brune, Fuller, and Smith (2010); Cyburt (2004); Cyburt, Fields, and Olive (2008); Cyburt and Pospelov (2012); Fields (2011); Iocco and Pato (2012); Kirsebom and Davids (2011); Nollett and Burles (2000); Wang et al. (2011) and references therein]. In the present case,

the use of a non-Maxwellian velocity distribution seems to worsen this scenario. A recent analysis yields the observational value of $^7$Li/H $= (1.58 \pm 0.31) \times 10^{-10}$ (Sbordone, 2010).

We have calculated a window of opportunity for the non-extensive parameter $q$ with which one can reproduce the observed abundance of light elements. We chose the data for the abundances, $Y_i$, of $^4$He/H, D/H, $^3$He/H and $^7$Li as reference. We then applied the ordinary $\chi^2$ statistics, defined by the minimization of

$$\chi^2 = \sum_i \frac{[Y_i(q) - Y_i(obs)]^2}{\sigma_i}, \tag{5.1}$$

where $Y_i(q)$ are the abundances obtained with the non-extensive statistics with parameter $q$, $Y_i(obs)$ are the observed abundances, and $\sigma_i$ the errors for each datum, and the sum is over all data mentioned in Table 5.1. From this chi-square fit we conclude that $q = 1^{+0.05}_{-0.12}$ is compatible with observations.

No attempt has been made to determine which element dominates the constraint on $q$. This might be important for a detailed study of the elemental abundance influence from nuclear physics inputs, namely, the uncertainty of the reaction cross sections. A study along these lines might be carried in a similar fashion as described in Nollett and Burles (2000). Weights on the reliability of observational data should also be considered for a more detailed analysis. For example, constraints arising from $^3$He/H abundance may not be considered trustworthy because of uncertain galactic chemical evolution. On the other hand, a constraint from the observation of $^3$He/D is more robust, and so on. Based on our discussion in Section II, it is more important to determine how the non-extensive statistics can modify more stringent conditions during the big bang, such as the modification of weak-decay rates and its influence on the n/p ratio which strongly affects the $^4$He abundance.

In Table 5.1 we present results for the predictions of the BBN with Maxwellian and non-Maxwellian distributions. The predictions are compared with data from observations reported in the literature. It is evident that the results obtained with the non-extensive statistics strongly disagree with the data. The overabundance of $^7$Li compared to observation gets worse if $q > 1$. The three light elements D, $^4$He and $^7$Li constrain the primordial

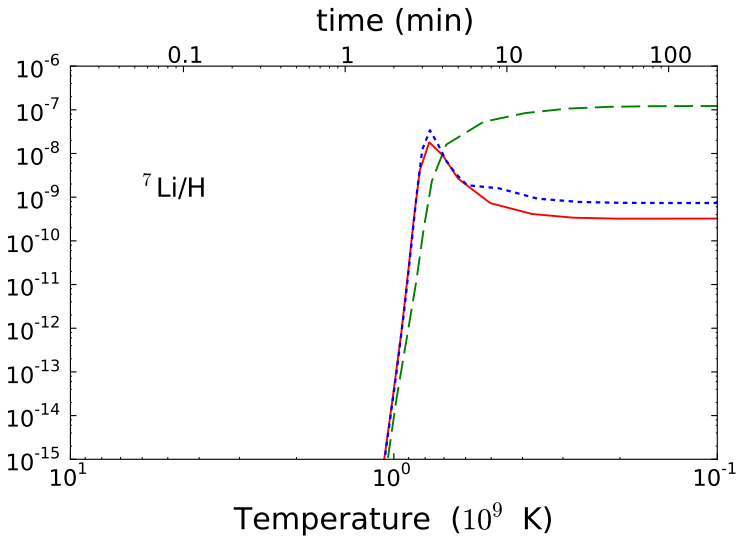


Figure 5.4: $^7$Li abundance. The solid curve is the result obtained with the standard Maxwell distributions for the reaction rates. Results with the use of non-extensive distributions for $q = 0.5$ (dotted line) and $q = 2$ (dashed line) are also shown.

abundances rather well. For all these abundances, a non-extensive statistics with $q > 1$ leads to a greater discrepancy with the experimental data.

Except for the case of $^3$He the use of non-extensive statistics with $q < 0.5$ does not rule out its validity when the non-Maxwellian BBN results are compared to observations. $^3$He is at present only accessible in our Galaxy's interstellar medium. This means that it cannot be measured at low metallicity, a requirement to make a fair comparison to the primordial generation of light elements. This also means that the primordial $^3$He abundance cannot be determined reliably. The result presented for the $^3$He abundance in Table 5.1 is quoted from Bania et al. (2002). Notice that our analysis does not include the changes that the non-extensive statistics would bring to the n/p conversion rates. The electron distributions would also be expected to change accordingly. This would change the freeze out temperature and a corresponding influence on the $^4$He abundance.

We conclude that it does not seem possible to change the Maxwell-Boltzmann statistics to reproduce the observed abundance of light elements in the universe without destroying many other successful predictions of big bang nucleosynthesis. A chi-square fit of our calculations with the observations of elemental abundance concludes that the non-extensive

parameter is constrained to $q = 1^{+0.05}_{-0.12}$. This means that, should a non-Maxwellian distribution due to the use of the Tsallis non-extensive statistics be confirmed (with a sizable deviation from $q = 1$), our understanding of the cosmic evolution of the universe would have to be significantly changed.

# REFERENCES


Ando, S., Cyburt, R., Hong, S., & Hyun, C. (2006). Radiative neutron capture on a proton at BBN energies. *Phys.Rev.*, *C74*, 025809. doi: 10.1103/PhysRevC.74.025809

Angulo, C. e. a. (1999). A compilation of charged-particle induced thermonuclear reaction rates. *Nucl.Phys.*, *A656*, 3-183.

Aragao-Rego, H. e. a. (2003). Bose-Einstein and Fermi-Dirac distributions in nonextensive Tsallis statistics: An Exact study. *Physica*, *A317*, 199. doi: 10.1016/S0378-4371(02)01330-4

A. Serebrov, A. K. e. a., V. Varlamov. (2005). Measurement of the neutron lifetime using a gravitational trap and a low-temperature fomblin coating. *Phys. Lett.*, *B605*, 72-78.

Aver, E., Olive, K. A., & Skillman, E. D. (2010). A New Approach to Systematic Uncertainties and Self-Consistency in Helium Abundance Determinations. *JCAP*, *1005*, 003. doi: 10.1088/1475-7516/2010/05/003

Bania, T., Rood, R. T., & Balser, D. S. (2002). The cosmological density of baryons from observations of 3He+ in the Milky Way. *Nature*, *415*, 54-57. doi: 10.1038/415054a

Bernui, A., Tsallis, C., & Villela, T. (2007). Deviation from Gaussianity in the cosmic microwave background temperature fluctuations. *Europhys.Lett.*, *78*, 19001. doi: 10.1209/0295-5075/78/19001

Bertulani, C. (2007). *Nuclear physics in a nutshell* (1st ed.). Princeton University Press.

Bertulani, C. A., Fuqua, J., & Hussein, M. (2013). Big bang nucleosynthesis with a non-maxwellian distribution. *ApJ*, *767*(67).

Boesgaard, A. M., & Steigman, G. (1985). Big Bang Nucleosynthesis: Theories and Observations. *Ann.Rev.Astron.Astrophys.*, *23*, 319-378.

Borchers, R., & Poppe, C. (1963). Neutrons from Proton Bombardment of Lithium. *Phys.Rev.*, *129*, 2679-2683. doi: 10.1103/PhysRev.129.2679

Bosch, H.-S., & Hale, G. (1992). Improved formulas for fusion cross-sections and thermal reactivities. *Nuclear Fusion*, *32*(4), 611.

Bouchet, F., Dauxois, T., & Ruffo, S. (2006, May). Controversy about the applicability of Tsallis statistics to the HMF model. *Europhysics News*, *37*.

Boyd, R. N., Brune, C. R., Fuller, G. M., & Smith, C. J. (2010). New Nuclear Physics for Big Bang Nucleosynthesis. *Phys.Rev.*, *D82*, 105005. doi: 10.1103/PhysRevD.82.105005

Brown, R. E., & Jarmie, N. (1990). Differential cross sections at low energies for H-2 (d,p) H-3 and H-2 (d, n) He-3. *Phys.Rev.*, *C41*, 1391-1400. doi: 10.1103/PhysRevC.41.1391

Buyukkilic, F., & Demirhan, D. (2000). A Unified grand canonical description of the nonextensive thermostatistics of the quantum gases: Fractal and fractional approach. *Eur.Phys.J.*, *B14*, 705. doi: 10.1007/s100510051082

Cassagnou, Y., Jeronymo, J. M., Mani, G. S., Sadeghi, A., & Forsyth, P. D. (1962). The li-7 (p, a) he-4 reaction. *Nucl. Phys.*, *33*, 449.

Cassagnou, Y., Jeronymo, J. M., Mani, G. S., Sadeghi, A., & Forsyth, P. D. (1963). The li-7 (p, a) he-4 reaction (erratum). *Nucl. Phys.*, *41*, 176.

Chamati, H., Djankova, A. T., & Tonchev, N. S. (2003, November). The black-body radiation in Tsallis statistics. *eprint arXiv:cond-mat/0311234*.

Chavanis, P., & Sire, C. (2005). On the interpretations of tsallis functional in connection with vlasov-poisson and related systems: Dynamics vs thermodynamics. *Physica A: Statistical Mechanics and its Applications*, *356*(2), 419-446.

Coc, A., Goriely, S., Xu, Y., Saimpert, M., & Vangioni, E. (2012). Standard Big-Bang Nucleosynthesis up to CNO with an improved extended nuclear network. *Astrophys.J.*, *744*, 158.

Collaboration, L. (2006). Precision electroweak measurements on the z resonance. *Physics Reports*, *427*, 257-545.

Coraddu, M. e. a. (1999). Thermal distributions in stellar plasmas, nuclear reactions and solar neutrinos. *Braz.J.Phys.*, *29*, 153-168.

C. Tsallis, M. G.-M., & Sato, Y. (2005). Asymptotically scale-invariant occupancy of phase space makes the entropy $s_q$ extensive. *Proc. Natl. Acad. Sci.*, *102*(43).

Cyburt, R. H. (2004). Primordial nucleosynthesis for the new cosmology: Determining uncertainties and examining concordance. *Phys.Rev.*, *D70*, 023505. doi: 10.1103/PhysRevD.70.023505

Cyburt, R. H., Fields, B. D., & Olive, K. A. (2008). An Update on the big bang nucleosynthesis prediction for Li-7: The problem worsens. *JCAP*, *0811*, 012.

Cyburt, R. H., & Pospelov, M. (2012). Resonant enhancement of nuclear reactions as a possible solution to the cosmological lithium problem. *Int.J.Mod.Phys.*, *E21*, 1250004. doi: 10.1142/S0218301312500048

Damian H. Zanette, e. a. (2003). Thermal measurements of stationary nonequilibrium systems: a test for generalized thermostatistics. *Phys. Lett. A*, *316*, 184-189.

da Silva, L., Lima, J., & Santos, J. (2000). Plasma oscillations and nonextensive statistics. *Phys.Rev.*, *E61*, 3260. doi: 10.1103/PhysRevE.61.3260

Dauxois, T. (2007). Non-gaussian distributions under scrutiny. *Journal of Statistical Mechanics: Theory and Experiment*(08), N08001.

Degl'Innocenti, S., Fiorentini, G., Lissia, M., Quarati, P., & Ricci, B. (1998). Helioseismology can test the Maxwell-Boltzmann distribution. *Phys.Lett.*, *B441*, 291-298. doi: 10.1016/S0370-2693(98)01125-3

Descouvemont, P., Adahchour, A., Angulo, C., Coc, A., & Vangioni-Flam, E. (2004). Compilation and R-matrix analysis of Big Bang nuclear reaction rates. *Atom.Data Nucl.Data Tabl.*.

Fa, K., & Lenzi, E. (2001). Exact equation of state for two-dimensional gravitating system within Tsallis statistical mechanics. *J.Math.Phys.*, *42*, 1148. doi: 10.1063/1.1335553

Fiedler, O., & Kunze, P. (1967). Wirkungsquerschnitte der kernreaktionen li-6 (p, a) he-3 und li-7 (p,a) he-4 bei kleinsten energien. *Nucl. Phys.*, *A96*, 513.

Fields, B. D. (2011). The primordial lithium problem. *Annu. Rev. Nucl. Part. Sci.*, *61*, 47-68.

Fowler, W., Caughlan, G., & Zimmerman, B. (1967). Thermonuclear reaction rates. *Ann. Rev. Astron. Astrophys.*, *5*, 525-570.

Gell-Mann, M., & Tsallis, C. (2004). *Nonextensive entropy-interdisciplinary applications*. Oxford University Press, New York.

Gibbons, J. H., & Macklin, R. L. (1959, Apr). Total neutron yields from light elements under proton and alpha bombardment. *Phys. Rev.*, *114*, 571–580. doi: 10.1103/PhysRev.114.571

G. S. Mani, e. a. (1964). Study of the reaction li-7 (p, a) he-4 up to 12 mev proton energy. *Nucl. Phys.*, *60*, 588-592.

Haubold, H., & Kumar, D. (2008). Extension of thermonuclear functions through the pathway model including Maxwell-Boltzmann and Tsallis distributions. *Astropart.Phys.*, *29*, 70-76. doi: 10.1016/j.astropartphys.2007.11.006

H. Spinka, T. T., & Winkler, H. (1971). Low-energy cross sections for li-7 (p, a) he-4 and li-6 (p, a) he-3. *Nucl. Phys.*, *A164*, 1.

(n.d.). Retrieved 2013, from `http://www.nndc.bnl.gov`

Iocco, F., Mangano, G., Meile, G., Pisanti, O., & Serpico, P. (2009, Mar). Primordial nucleosynthesis: From precision cosmology to fundamental physics. *Phys. Rep.*, *472*, 1-76.

Iocco, F., & Pato, M. (2012). Lithium synthesis in microquasar accretion. *Phys.Rev.Lett.*, *109*, 021102. doi: 10.1103/PhysRevLett.109.021102

Izotov, Y., & Thuan, T. (2010). The primordial abundance of 4He: evidence for non-standard big bang nucleosynthesis. *Astrophys.J.*, *710*, L67-L71. doi: 10.1088/2041-8205/710/1/L67

J.M. Freeman, e. a. (1958). The nuclear reaction he-4 (a, p) li-7 and its inverse. *Nucl. Phys.*, *5*, 148.

Joakim Brorsson, e. a. (2010). Big bang nucleosynthesis.

Kaniadakis, G., Lissia, M., & Scarfone, A. (2005). Two-parameter deformations of logarithm, exponential, and entropy: a consistent framework for generalized statistical mechanics. *Phys.Rev.*, *E71*, 046128. doi: 10.1103/PhysRevE.71.046128

Kawano, L. (1988). *Fermilab report no. pub-88/34-a.*

Kawano, L. (1992).

*NASA STI/Recon Technical Report N*, *92*(25163).

Kirsebom, O., & Davids, B. (2011). One fewer solution to the cosmological lithium problem. *Phys.Rev.*, *C84*, 058801. doi: 10.1103/PhysRevC.84.058801

Koehler, P. e. a. (1988). Be-7 (n, p) Li-7 total cross section from 25 meV to 13.5 keV. *Phys.Rev.*, *C37*, 917-926. doi: 10.1103/PhysRevC.37.917

Komatsu, E. e. a. (2011). Seven-year wilkinson microwave anisotropy probe (wmap) observations: Cosmological interpretation. *ApJS*, *192*.

Kraushaar, e. a., J. (1984). Energy and problems of a technical society.

Krauss, A., Becker, H., Trautvetter, H., Rolfs, C., & Brand, K. (1987). Low-energy fusion cross sections of d + d and d + 3he reactions. *Nuclear Physics A*, *465*(1), 150 - 172.

Lerner, G. M., & Marion, J. B. (1969). Measurement of (p, p) and (p, a) cross sections for lithium and fluorine. *Nucl. Instr. Meth.*, *69*, 115.

Lima, J., Silva, R., & Santos, J. (2002). Jeans' gravitational instability and nonextensive kinetic theory. *Astron.Astrophys.*, *396*, 309-314. doi: 10.1051/0004-6361:20021395

Lissia, M., & Quarati, P. (2005). Nuclear astrophysical plasmas: ion distribution functions and fusion rates. *Europhys.News*, *36*, 211-214. doi: 10.1051/epn:2005610

Mathews, G. J., Kajino, T., & Shima, T. (2005, Jan). Big bang nucleosynthesis with a new neutron lifetime. *Phys. Rev. D*, *71*, 021302.

Muñoz, V. (2006). A nonextensive statistics approach for langmuir waves in relativistic plasmas. *Nonlinear Processes in Geophysics*, *13*(2), 237–241.

Nauenberg, M. (2003). Critique of q-entropy for thermal statistics. *Phys.Rev.*, *E67*, 036114. doi: 10.1103/PhysRevE.67.036114

Nollett, K. M., & Burles, S. (2000). Estimating reaction rates and uncertainties for primordial nucleosynthesis. *Phys.Rev.*, *D61*, 123505. doi: 10.1103/PhysRevD.61.123505

Olive, K. A. (2002). Big bang nucleosynthesis, implications of recent cmb data and supersymmetric dark matter. , 23-62. Retrieved from `http://arxiv.org/abs/astro-ph/0202486`

Pessah, M., Torres, D. F., & Vucetich, H. (2001). Statistical mechanics and the description of the early universe. 1. Foundations for a slightly nonextensive cosmology. *Physica*, *A297*, 164-200. doi: 10.1016/S0378-4371(01)00235-7

Pettini, M. e. a. (2008). Deuterium abundance in the most metal-poor damped lyman alpha system: Converging on omega baryons.

P. Noterdaeme, R. S. e. a., P. Petitjean. (2011). Constraints on a vacuum energy from both snia and cmb temperature observations. *Astronomy and Astrophysics*.

Poppe, C., Anderson, J., Davis, J., Grimes, S., & Wong, C. (1976). Cross sections for the Li-7 (p, n) Be-7 reaction between 4.2 and 26 MeV. *Phys.Rev.*, *C14*, 438-445. doi: 10.1103/PhysRevC.14.438

Reichl, L. E. (2009). *A modern course in statistical physics*. Wiley-VCH Verlag GmbH.

Rényi, A. (1960). On measures of information and entropy. *Proc. of the 4th Berkeley Symposium on Mathematics, Statistics and Probability*, 547-561.

Rolfs, C., & Kavanagh, R. (1986). The li-7 (p, a) he-4 cross section at low energies. *Nuclear Physics A*, *455*(1), 179 - 188.

Sakagami, M., & Taruya, A. (2004). Self-gravitating stellar systems and non-extensive thermostatistics. *Continuum Mechanics and Thermodynamics*, *16*, 279-292. doi: 10.1007/s00161-003-0168-7

Sbordone, L. e. a. (2010). The metal-poor end of the Spite plateau. 1: Stellar parameters, metallicities and lithium abundances. *Astron.Astrophys.*, *522*, A26. doi: 10.1051/0004-6361/200913282

Schulte, R., Cosack, M., Obst, A., & Weil, J. (1972). 2h + reactions from 1.96 to 6.20 mev. *Nuclear Physics A*, *192*(3), 609 - 624. doi: 10.1016/0375-9474(72)90093-0

Sekharan, K. (1976, March). A neutron detector for measurement of total neutron production cross sections. *Nuclear Instruments and Methods*, *133*, 253-257. doi: 10.1016/0029-554X(76)90617-0

S. Engstler, e. a. (1992a). Isotopic dependence of electron screening in fusion reactions. *Z. Phys A*, *342*, 471-482.

S. Engstler, e. a. (1992b). Test for isotopic dependence of electron screening in fusion reactions. *Phys. Lett. B*, *279*, 20-24.

Silva, R., Plastino, A., & Lima, J. (1998). A Maxwellian path to the q-nonextensive velocity distribution function. *Phys.Lett.*, *A249*, 401-408. doi: 10.1016/S0375-9601(98)00710-5

Smith, M. S., Kawano, L. H., & Malaney, R. A. (1993). Experimental, computational, and observational analysis of primordial nucleosynthesis. *Astrophys.J.Suppl.*, *85*, 219-247. doi: 10.1086/191763

Sokmen, I., Buyukkilic, F., & Demirhan, D. (2002). Nonextensive thermostatistical investigation of the blackbody radiation. *Chaos, Solitons and Fractals*, *13*(4), 749-759.

Taruya, A., & Sakagami, M.-a. (2003). Long - term evolution of stellar self - gravitating system away from the thermal equilibrium: Connection with non-extensive statistics. *Phys.Rev.Lett.*, *90*, 181101. doi: 10.1103/PhysRevLett.90.181101

Touchette, H. (2013, January). Comment on "Towards a large deviation theory for strongly correlated systems". *Physics Letters A*, *377*, 436-438.

Tsallis, C. (1988). Possible generalization of boltzmann-gibbs statistics. *Journal of Statistical Physics*, *52*(1-2), 479–487. doi: 10.1007/BF01016429

Tsallis, C. (2004, Mar). Comment on "critique of $q$ -entropy for thermal statistics". *Phys. Rev. E*, *69*, 038101. doi: 10.1103/PhysRevE.69.038101

Tsallis, C. (2009). *Introduction to nonextensive statistical mechanics.* Springer Verlag.

U. Greife, e. a. (1995). Oppenheimer-phillips effect and electron screening in d+d fusion reactions. *Z. Phys A*, *351*, 107-112.

Vangioni-Flam, E., Olive, K. A., Fields, B. D., & Casse, M. (2003). On the baryometric status of He-3. *Astrophys.J.*, *585*, 611-616. doi: 10.1086/346232

Wagoner, R. V., Fowler, W. A., & Hoyle, F. (1967). On the Synthesis of elements at very high temperatures. *Astrophys.J.*, *148*, 3-49. doi: 10.1086/149126

Wang, B., Bertulani, C., & Balantekin, A. (2011). Electron screening and its effects on Big-Bang nucleosynthesis. *Phys.Rev.*, *C83*, 018801. doi: 10.1103/PhysRevC.83.018801

Werby, M. F. e. a. (1973). Study of alpha+d and he-3+t clustering in li-6 with a two-mode, finite-range analysis of the li-6 (p, he-3) he-4 reaction. *Phys. Rev.*, *C8*, 106-113.

Wietfeldt, F. E., & Greene, G. L. (2011, Nov). *Colloquium* : The neutron lifetime. *Rev. Mod. Phys.*, *83*, 1173-1192.

Zanette, D. H., & Montemurro, M. A. (2004, April). A note on non-thermodynamical applications of non-extensive statistics. *Physics Letters A*, *324*, 383-387. doi: 10.1016/j.physleta.2004.03.024

# VITA

John Fuqua attended Detroit High School in Detroit, Texas where he earned his diploma in 2007. At this time he entered Texas A&M University-Commerce and went on to complete a Bachelor of Science in Physics in December of 2010. He then enrolled in the Physics graduate program at Texas A&M University-Commerce. Permanent address:

Department of Physics & Astronomy
Texas A&M University-Commerce
2600 South Neal Street
Commerce, TX 75428